Universidade de Aveiro Departamento de Química

2011

Tiago Filipe Cruz Carvalho

Efeito da diabetes *mellitus* tipo 1 na função mitocondrial

Type 1 diabetes *mellitus* effects on mitochondrial function

Universidade de Aveiro Departamento de Química

2011

Tiago Filipe Cruz Carvalho

Efeito da diabetes *mellitus* tipo 1 na função mitocondrial

Type 1 diabetes *mellitus* effects on mitochondrial function

Dissertação apresentada à Universidade de Aveiro para cumprimento dos requisitos necessários à obtenção do grau de Mestre em Bioquímica com especialização em Métodos Biomoleculares, realizada sob a orientação científica do Doutor Francisco Manuel Lemos Amado, Professor Associado do Departamento de Química da Universidade de Aveiro e da Doutora Rita Maria Pinho Ferreira, Professora Auxiliar do Departamento de Química da Universidade de Aveiro

Apoio financeiro da FCT
(PTDC/QUI/72683/2006)

Dedico este trabalho aos meus pais e ao meu irmão, que sempre me apoiaram e fizeram ser possível aqui chegar.

o júri
presidente

Prof. Doutor Pedro Miguel Dimas Neves Domingues
Professor auxiliar do departamento de química da Universidade de Aveiro

Prof. Doutora Maria João Garrett Silveirinha Sottomayor Neuparth
Professora coordenadora do Instituto Politécnico de Saúde Norte, CESPU.

Prof. Doutor Francisco Manuel Lemos Amado
Professor associado do departamento de química da Universidade de Aveiro

Prof. Doutora Rita Maria Pinho Ferreira
Professora auxiliar convidada do departamento de química da Universidade de Aveiro

agradecimentos

Aos meus orientadores Doutor Francisco Amado e Doutora Rita Ferreira pela orientação, pelo voto de confiança, pelo conhecimento transmitido e pelas criticas construtivas ao longo do trabalho.

Ao Doutor Rui Vitorino por toda a indispensável ajuda e orientação ao nível laboratorial e técnico.

À Ana Padrão pelas dicas e por toda a preciosa ajuda tanto na parte laboratorial, como na parte escrita desta tese.

Ao Renato Alves pelos bons conselhos e por toda a ajuda dada ao longo da parte prática deste trabalho.

Aos meus colegas de mestrado Ana, Cátia, David, Gabriela, Igor, Isabel, João, Luísa, Miguel, Raquel e Tânia pelo apoio e bons momentos passados durante este ano.

A todos os restantes membros do grupo de espectrometria de massa, de que alguma forma ajudaram ao longo deste percurso, tanto pela disponibilidade, ajuda e pelo bom ambiente que criaram.

palavras chave

diabetes *mellitus* do tipo 1, g*astrocnemius,* subpopulações mitocondriais, complexos da fosforilação oxidativa, proteínas da superfamília AAA^{+}.

resumo

Apesar de a diabetes tipo 1 ser uma das formas mais raras de diabetes *mellitus*, tem uma origem auto-imune e aparece precocemente na vida de um indivíduo afectando grandemente a qualidade da mesma. No sentido de melhor compreender os mecanismos moleculares subjacentes às alterações fenotípicas observadas no músculo esquelético dos pacientes diabéticos, delineou-se um protocolo experimental com 20 ratos Wistar com 8 semanas de idade, aleatoriamente divididos em dois grupos (n=10). Os animais de um dos grupos foram injectados com 60mg/Kg de streptozotocina (STZ), e os outros com veículo. Após 4 meses, os ratos injectados com STZ foram confirmados como diabéticos, tendo em consideração a hiperglicemia e a perda de massa corporal. Após o sacrifício dos animais foram retirados os músculos *gastrocnemius*, a partir dos quais foram isoladas as duas subpopulações mitocondriais (subsarcolemal (SS) e intermiofibrilar (IMF)). A análise da razão mtADN-massa muscular sugere que a administração de STZ induziu o aumento da biogénese mitocondrial SS associado a um decréscimo do teor proteico mitocondrial, ao contrário do observado nas mitocôndrias IMF. O perfil de BN-PAGE revelou uma ligeira diferença entre a organização dos complexos da fosforilação oxidativa entre ambas as subpopulações mitocondriais, aparentemente não afectada pela administração de STZ. A análise da proteólise mitocondrial, efectuada por zimografia, evidenciou duas proteases com 15 e 25 KDa, tendo-se observado uma diminuição acentuada da actividade da protease com menor peso molecular nas mitocôndrias IMF dos animais diabéticos. Uma tendência semelhante foi observada para a expressão da subunidade paraplegina do sistema proteolítico m-AAA e para a mitofilina, uma proteína envolvida na organização da membrana interna mitocondrial. Curiosamente, nas mitocôndrias SS dos animais diabéticos verificaram-se níveis mais elevados destas proteínas.

Com este estudo verificou-se que no *gastrocnemius*, as mitocôndrias IMF são mais afectadas pela diabetes *mellitus* tipo 1 do que as SS. A diminuição da actividade do sistema de controlo da qualidade proteica parece estar associada às alterações morfológicas e bioquímicas observadas nas mitocôndrias localizadas entre as fibrilas.

keywords

type 1 diabetes *mellitus, gastrocnemius* muscle, mitocondrial subpopulations, oxidative phosphorilation complexes, superfamily of AAA^+ proteins.

abstract

Despite type 1 diabetes *mellitus* being more rare, it has an autoimmune origin and appears early in life, greatly affecting its quality. With the aim of better understand the molecular mechanisms underlying the observed phenotypic alterations in the skeletal muscle from diabetic patients, it was planned an experimental protocol using 20 Wistar rats 8 weeks old, randomly divided in two groups (n=10). The animals from one group were injected with 60mg/Kg of streptozotocin (STZ), while the others were injected with vehicle buffer. Four months after STZ injection, rats were confirmed as diabetic, considering hyperglycemia and body weight loss. After animals sacrifice, *gastrocnemius* muscles were excised and used for mitochondria subpopulations (subsarcolemmal (SS) and intermyofibrillar (IMF)) isolation. mtDNA-to-muscle mass ratio suggest an increased biogenesis of SS mitochondria in the STZ animals, paralleled by a decreased protein content per mitochondrion, in opposite to the observed in IMF mitochondria. The BN-PAGE profile revealed a slight difference of the oxidative phosphorylation complexes organization between mitochondrial subpopulations, apparently not affected by STZ administration. Mitochondrial proteolysis analysis, evaluated through zymography, revealed two proteases with molecular weights around 15 and 25 KDa, with the smaller one presenting STZ-induced significant decreased activity in IMF mitochondria. A similar behavior was observed for paraplegin, a subunit of m-AAA proteolytic system, and mitofilin, a protein involved in cristae organization. Interestingly, these protein levels were higher in SS mitochondria from diabetic animals.

With this work it was verified that subsarcolemmal mitochondria are not so affected by STZ administration as IMF mitochondria. The decreased activity of the protein quality control system seems to be associated with the morphological and biochemical alterations observed in the mitochondria interspersed in fibrils.

Index

1. Introduction 1

1.1. Mitochondrial origin, structure and function 3

1.2. Mitochondrial OXPHOS complexes organization 4

1.3. Protein quality control within mitochondria: the role of mitochondrial proteases.....8

1.3.1. Regulation of mitochondrial cristae morphology 12

1.4. Mitochondrial biogenesis in the striated muscle.....13

1.5. Mitochondrial impairment in type 1 diabetes *mellitus* 16

1.6. Objectives 18

2. Material and Methods.....19

2.1. Animals.....20

2.2. Isolation of SS and IMF mitochondrial subpopulations 20

2.3. Electron microscopic analysis and average mitochondrial area calculation.....21

2.4. BN-PAGE and in-gel activity of OXPHOS complexes IV and V.....22

2.5. Protease activity analysis through gelatin zymography.....23

2.6. Proteases identification from zymography and SDS-PAGE gels.....23

2.7. Western Blot analysis 25

2.8. Statistical analysis 25

3. Results 27

3.1. Validation of the experimental T1DM animal model 28

3.2. Evaluation of mtDNA and mitochondrial protein concentrations in skeletal muscle 29

3.3. Morphological characterization of mitochondrial subpopulations 30

3.4. BN-PAGE and in gel activity of OXPHOS complexes IV and V 31

3.5. Gelatin zymography analysis 33

3.6. Western blot analysis 34

4. Discussion 37

5. Conclusions 43

6. References 47

Figures index

Figure 1: Schematic representation of mitochondria and its compartments [10]..... 3

Figure 2: Representation of the electron transport chain within mitochondria, where the succinate and the NADH produced in citric acid cycle, give their electrons whose enter in an electron flow, with the final objective to produce ATP. Adapted from [25]..... 5

Figure 3: QC applied to mitochondrial proteins. ATP-dependent proteases present in various mitochondrial compartments recognize non-native polypeptides and trigger their proteolysis to peptides that are further degraded by oligopeptidases. At the same time, energy-dependent proteases can act as processing enzymes ensuring assembly and integrity of OXPHOS complexes [31]..... 9

Figure 4: QC proteases monitor the four mitochondrial compartments. Localized QC proteases monitor and protect all four mitochondrial compartments against deleterious accumulation of misfolded, misassembled or unfolded proteins [38].. 10

Figure 5: Regulation of OXPHOS complexes assembly and maintenance by proteases. (a) The assembly of mitochondrial ribosomes and synthesis of mitochondrially encoded RC subunits require maturation of newly imported MrpL32 by the m-AAA protease. (b) Biogenesis of the ROS scavenger Ccp1 in yeast mitochondria depends on ATP-dependent membrane dislocation of the precursor protein by the m-AAA protease and maturation by the rhomboid protease Pcp1 [31]. 11

Figure 6: Contractile activity-induced molecular adaptations within skeletal muscle which lead to IMF and SS mitochondrial biogenesis and the expression of nuclear genes encoding mitochondrial proteins (NUGEMPs) [64]. 14

Figure 7: Osmium-extracted mitochondria. Strands in background are ribbons of agarose. (a): Cluster of SS with solely lamelliform cristae. Scale bar, 1μm. (b): SS

with mostly lamelliform cristae. Scale bar, 0.5μm. (c): IMF with exclusevely tubular cristae. Scale bar, 0.5 μm. (d): IMF with mainly lamelliform cristae. Scale bar, 0.5μm [65]. 15

Figure 8: Organization of SS mitochondrial clusters in rat *soleus* muscle. Clusters of subsarcolemmal mitochondria are densely packed. Mitochondria located near the outer cell membrane demonstrate interconnections and mitochondrial network (arrows), whose are necessary to synchronize mitochondrial activities between contractions cycles and to share the metabolic feedback regulation of mitochondrial respiration via energy transfer networks. *Soleus* mitochondria were labeled with Rhod-2. Scale bars, 5 μm [63]. 16

Figure 9: Relationship between mitochondrial protein folding, metabolism and dysfunction. Mitochondrial protein homeostasis depend upon a balance between deleterious aspects of cellular and organelle biology that can produce large amounts of misfolded proteins (blue boxes) and the protective mechanisms such as the QC machinery and the mitochondrial upregulation (UPR^{mt}), that protect against the accumulation of misfolded or damaged proteins (orange boxes) [38]. 17

Figure 10: Percoll gradient loaded with crude mitochondrial after ultracentrifugation. Density differences are evident between SS and IMF subpopulations, for both groups in study (CONT and T1DM). No visible differences are noticed between mitochondria from control and T1DM groups. ... 30

Figure 11: TEM images from: (a) SS mitochondria from control rats, (b) SS mitochondria from T1DM rats, (c) IMF mitochondria from control rats and (d) IMF mitochondria from T1DM rats, with a magnification of 10,000x. (e) Box and whiskers graph where the mitochondrial area of the different populations is compared (n=180 for SS and n=800 for IMF). Scale bar = 2 μm. 31

Figure 12: BN-PAGE profile of SS and IMF mitochondria. An overlap of the density variation of the four lanes is presented on the right. 32

Figure 13: Effects of T1DM in the in-gel activity of respiratory chain complexes IV (a) and V (c) of mitochondrial subpopulations SS and IMF, with respective

representative images (b+d). The OD results are expressed in arbitrary units (mean ± standard deviation). 33

Figure 14: Effects of T1DM in the proteolytic activity of mitochondrial subpopulations (SS and IMF) (a) Representative image of the zymography evidencing two light bands with noticeable proteolytic activity. Comparison of OD variation for each band: the upper band (b) and the lower band (c). The OD results are expressed in arbitrary units (mean ± standard deviation). 34

Figure 15: (a) Effects of T1DM in the ATP synthase expression in the different mitochondrial subpopulations. The OD results are expressed in arbitrary units (mean ± standard deviation). (b) Representative image of the Western blot. 35

Figure 16: Effects of T1DM in paraplegin expression in the different mitochondrial subpopulations (SS and IMF). The OD results are expressed in arbitrary units (mean ± standard deviation). (b) Representative image of the Western blot. 35

Figure 17: Effects of T1DM in mitofilin expression, in IMF mitochondrial subpopulation,. The OD results are expressed in arbitrary units (mean ± standard deviation). (b) Representative image of the Western blot. 36

Tables Index

Table 1: Mitochondrial genome codified proteins from Rattus *norvegicus*. List obtained from Genome database (http://www.ncbi.nlm.nih.gov/sites/entrez), access number NC_001665. 5

Table 2: Glicemia and HbA1c measured values for each group (control and type 1 diabetes). The values are presented with mean ± standard deviation. 28

Table 3: The effect of T1DM in rat body weight, *gastrocnemius* muscle mass and *gastrocnemius* muscle/ body weight ratio. The values are presented with mean ± standard deviation. 28

Table 4 Effects of T1DM in mitochondrial protein content-to-mtDNA concentration, mtDNA-to-muscle mass and protein content-to-muscle mass. The results are expressed as mean ± standard deviation. 29

Abbreviations

AAA^+ - ATPases associated with a variety of cellular activities

BN – Blue native

Ccp1 - cytochrome c peroxidase

CI – Complex I

CII - Complex II

CIII - Complex III

CIV - Complex IV

CoQ – Coenzyme Q

CV - Complex V

CytC – Cytochrome C

DNA – Deoxyribonucleic acid

EB – Extraction buffer

EGTA - Ethylene glycol-bis(2-aminoethylether)-*N*,*N*,*N′*,*N′*-tetraacetic acid

ETC – Electron transport chain

HSP - Hereditary spastic paraplegia

IM – Inner membrane

IMF – Intermyofibrillar

IMS – Intermembrane space

KDa - Kilodalton

MALDI – Matrix-assisted laser desorption/ionization

MOPS - 3-(N-morpholino)propanesulfonic acid

MS – Mass spectrometry

mtDNA – Mitochondrial DNA

MW – Molecular weight

NADH – Nicotinamide adenine dinucleotide

OD – Optical density

OM – Outer membrane

PAGE – Polyacrylamide gel electrophoresis

QC – Quality control

RNA – Ribonucleic acid

SB – Sucrose buffer

SS – Subsarcolemmal

STZ - Streptozotocin

T1DM - Type 1 diabetes *mellitus*

TBS – Tris-buffered saline

TEM – Transmission electron microscopy

TFAM – Transcription factor A, mitochondrial

TOF – Time of flight

tRNA – Transfer RNA

TTBS – TBS with Tween-20

UPR^{mt} - mitochondrial upregulation response

1. Introduction

In 2010, it was estimated that 6.4% of the world adult population was affected with diabetes *mellitus*. This number is expected to increase year by year, reaching, in 2030, 7.7% of the adult population, being one of the major causes of premature illness and death worldwide [1]. This reality has motivated several studies in order to comprehend the molecular mechanisms involved in this pathophysiology [2]. Type 1 diabetes *mellitus* (T1DM) is not the biggest responsible for these numbers, neither the most studied type of diabetes mellitus, but since it has an autoimmune origin, and its patients have decreased life quality [3], it seems urgent to better understand this disease.

The diagnosis of T1DM is made through evident first signs like polyuria, weight loss and the constant tiredness, these signs are related with the high concentration of blood glucose and the lack of cell glucose, needed for energy production [4]. To compensate this glucose deficit, cell metabolizes lipids in order to produce the needed energy, which in advanced phases of T1DM causes diabetic ketoacidosis [5]. The treatment consists in the injection of insulin, in order to regulate the blood levels of glucose [4], which should be accompanied with appropriate physical exercise and low carbohydrate diets [6]. When not treated, T1DM can cause serious complications like cerebral stroke, renal failure, visual problems, including blindness, difficult to heal injuries and even myocardial infarction [5].

Due to its metabolic dependence on insulin, skeletal muscle is one of the most affected organs by T1DM, which account for 42% of body weight. In order to better understand the molecular pathways involved in muscle T1DM-induced functional alterations which compromise patients' quality of life [7], studies focused on muscle bioenergetic alterations and associated regulatory mechanisms seem urgent [8]. Mitochondria play a very important role in the skeletal muscle bioenergetics, making them an appellative target of study focused on skeletal muscle physiopathologies like diabetes.

1.1. Mitochondrial origin, structure and function

Mitochondria are essential cellular organelles that provide the majority of the energy necessary for cell and tissue functions. It is present in all eukaryotic cells, and a typical human cell has several hundreds of mitochondria [9]. Mitochondria size range between 0.5-1 µm and have two membranes. The outer membrane is smooth and contains several transport proteins, which forms aqueous channels allowing some molecules to penetrate the membrane. The inner membrane is formed by multiple invaginations, forming the cristae which can be tubular or lamellar (Figure 1).

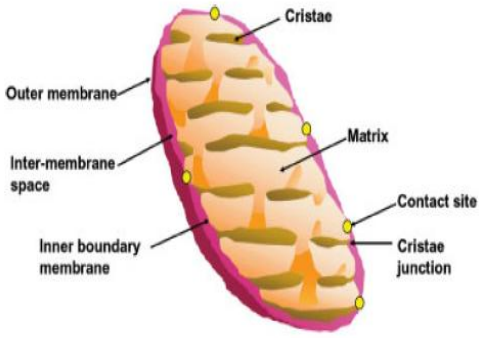

Figure 1: Schematic representation of mitochondria and its compartments [10].

Currently, the most accepted theory of mitochondrial origin is that present mitochondria are a remnant of a symbiotic relationship between a prokaryotic organism and another cell, creating the eukaryotic cell [11]. In 1997, Lang *et al.* [12] studied the protozoon *Reclinomonas americana*, which has the most similar genome to mitochondria. One year later, in 1998, Andersson *et al.* [13] studied *Rickettsia prowazekii* the most mitochondria-like eubacterial genome. Current theories also state that no eukaryote exists without mitochondria in it, indicating that the insertion of the symbiont protobacteria into the anaerobic host effectively improved respiration, causing them to sustain this symbiotic relationship [9; 11].

Mitochondria produce energy through a metabolic pathway composed by five complexes, called the oxidative phposphorylation (OXPHOS), which occurs in the mitochondrial inner membrane that surrounds the matrix space of each mitochondrion. This organelle matrix contains mitochondrial DNA (mtDNA),

tRNAs, ribosomes and various enzymes used for protein synthesis, pyruvate oxidation, for the citric acid cycle and for the oxidation of fatty acids which combined with other proteins makes about 1500 proteins per mitochondrion, most of which encoded in the nucleus [10; 14]. Mitochondria are also responsible for several other important functions like heat production, calcium storage and signaling contributing for cell's homeostasis, regulation of the cell membrane potential, cell apoptosis, cellular proliferation and metabolism, steroids synthesis and certain heme synthesis reactions [15; 16; 17].

Since mitochondria are the main ATP suppliers of the cell, they have a very important role in cellular metabolism, cell apoptosis and are the largest producers of ROS in the organism, which has a significant role in the aging process [18; 19; 20]. Therefore, any disturbance in mitochondrial homeostasis, will compromise the cell's homeostasis or, if a tissue suffers any disturbance, mitochondria will have to adapt to balance its homeostasis [18; 21; 22]

1.2. Mitochondrial OXPHOS complexes organization

OXPHOS is a cellular pathway which consists in the activity of five complexes, with about 90 already known protein subunits [23]. Most of these subunits are encoded in the nuclear genome, while 13 of them are encoded in the mtDNA [24] (Table 1).

Table 1: Mitochondrial genome codified proteins from Rattus *norvegicus*. List obtained from Genome database (http://www.ncbi.nlm.nih.gov/sites/entrez), access number NC_001665.

Codified protein	Length	GeneID	Locus
NADH dehydrogenase subunit 1	318	26193	ND1
NADH dehydrogenase subunit 2	346	26194	ND2
cytochrome c oxidase subunit I	514	26195	COX1
cytochrome c oxidase subunit II	227	26198	COX2
ATP synthase F0 subunit 8	67	26196	ATP8
ATP synthase F0 subunit 6	226	26197	ATP6
cytochrome c oxidase subunit III	261	26204	COX3
NADH dehydrogenase subunit 3	115	26199	ND3
NADH dehydrogenase subunit 4L	98	26200	ND4L
NADH dehydrogenase subunit 4	459	26201	ND4
NADH dehydrogenase subunit 5	609	26202	ND5
NADH dehydrogenase subunit 6	172	26203	ND6
cytochrome b	380	26192	CYTB

These OXPHOS complexes are located in the inner mitochondrial membrane, and are organized as described in Figure 2.

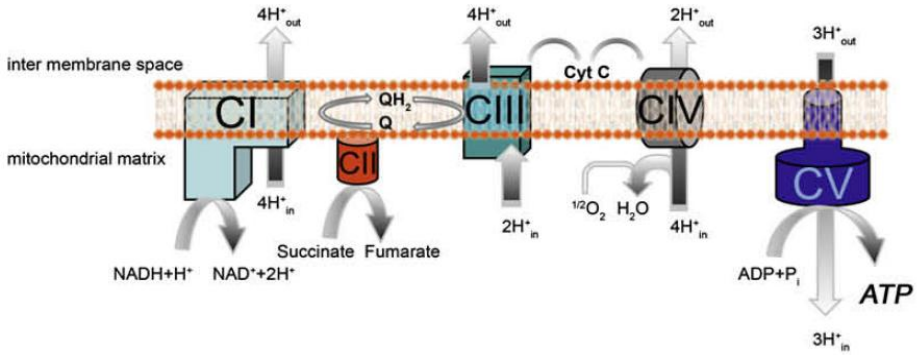

Figure 2: Representation of the electron transport chain within mitochondria, where the succinate and the NADH produced in citric acid cycle, give their electrons whose enter in an electron flow, with the final objective to produce ATP. Adapted from [25].

Resulted products from citric acid cycle, fatty acid β-oxidation and amino-acid oxidation, are used to produce ATP within mitochondria. At the mitochondrial inner membrane, electrons from reduced nicotinamide adenine dinucleotide (NADH) and succinate are transferred, respectively to complex I (CI) and complex II (CII), starting the electron transport chain (ETC). The ETC comprises an enzymatic series of electron donors and acceptors. Each electron donor passes electrons to a more electronegative acceptor, which in turn donates these electrons to another acceptor, a process that continues down the series until electrons are passed to oxygen, the most electronegative and terminal electron acceptor in the chain, which is reduced to water. Both complexes I and II transfer their pair of electrons to complex III (CIII), using coenzyme Q (CoQ) as intermediate receptor. Cytochrome c (CytC) also works as mobile carrier of electron, transporting them from CIII to complex IV (CIV), which one gives electron to the final receptor, the oxygen, reducing it into water. In each ETC complex, passages of electrons between donor and acceptor releases energy, which is used to generate a proton gradient across the mitochondrial membrane by actively pumping protons into the intermembrane space, producing a thermodynamic state that has the potential to do work. This potential created by an increased concentration of H^+ in the intermembranar space will be used by complex V (CV) to produce ATP, through the passage of these protons back into the mitochondrial matrix. A small percentage of electrons do not complete the whole series and instead directly leak to oxygen, resulting in the formation of ROS [25; 26; 27].

The organization of the respiratory chain complexes within the lipid bilayer is still not fully known. There are two main explanations for the interactions between complexes: the fluid state and the solid state models. The fluid state organization model supports that all five complexes exist as independent complexes which randomly diffuse within the lipid bilayer. Electron transfer between the complexes is supported through their collisions while diffusing in the membrane, and where coenzyme Q and cytochrome c, would exhibit faster diffusion rates relative to the larger membrane-embedded, multisubunit complexes. On the other hand, the solid state favors that a higher-level of organization of the OXPHOS complexes exists within the inner membrane which promotes directed electron channeling between physically associated OXPHOS complexes [28]. Studies where

the purifications of the OXPHOS complexes was performed with detergents into their individually active forms, demonstrates that their co-association in the membrane is not necessary for their enzymatic function [28]. However, a number of independent studies have demonstrated that the mitochondrial OXPHOS complexes can be co-purified together when solubilized from the mitochondrial membranes with detergents like digitonin [29]. The demonstration of purified OXPHOS supercomplexes formed by the physical association of proteins between these complexes and thus uniting them into a higher level of organization, favors that the OXPHOS complexes are not randomly organized as individual complexes in the membrane, as the liquid state model would predict, proposing that the different respiratory complexes are assembled into supramolecular structures, called supercomplexes, to perform their role [28]. The solid state model is sustained almost exclusively on consistent and repetitive observations showing the electrophoretic comigration of different respiratory complexes using native gels or centrifugation density gradients [25]. Since all the respiratory complexes are integral components of the mitochondrial inner membrane, their extraction requires the disorganization of this membrane. It has been reported that the more abundant, stable, and more easily purified supercomplex contains complexes I and III but not complex IV, and hence its functional role is difficult to envision, although the association of complex II in supercomplexes, has never been described [30]. Furthermore, it remains to be proved that the electrons are transferred between complexes within the supercomplex and, more important, that the supercomplexes containing CI, CIII, and CV are able to take electrons from NADH and use them to reduce oxygen. Therefore, the existence of respiratory supercomplexes in mitochondria as functional entities is far from being demonstrated [25].

Due to its role in cell bioenergetics, this complex mitochondrial machinery needs to be under tight control, being protein quality control systems of major importance in this process.

1.3. Protein quality control within mitochondria: the role of mitochondrial proteases

Protein quality control (QC) system within mitochondria has a great importance for cell survival, because when seriously damaged mitochondria produce more ROS, having low productivity in ATP synthesis [31] and may release pro-apoptotic proteins, inducing cell apoptosis [32].

Protein QC provides the first line of defense within mitochondria, being a highly conserved proteolytic system [33]. Molecular chaperones and energy-dependent proteases monitor the folding and assembly of mitochondrial proteins and selectively remove excess and damaged proteins from the organelle [31]. A second line of defense is provided at the organellar level by the dynamic nature of the mitochondrial population of a cell, where the functionality of damaged mitochondria can be restored by fusion with neighboring undamaged mitochondria [34].

The mitochondrial QC system has both the function of monitoring newly synthesized proteins proper folding and correct assembly, and selectively recognizing non-native, misfolded or non-assembled proteins, in order to remove and degrade them [31; 35]. The proteases from the QC quality control system, degrade damaged proteins to peptides, which are subsequently either exported from the organelle or degraded further to amino acids by various oligopeptidases (Figure 3) [31]. The protein folding and its proper function depends on each other, being the first one monitored as soon as the protein is synthesized, ant takes place in all cellular compartments [36]. Damaged proteins are mainly a consequence of ROS production, mutations or misfoldings, being its removal and degradation a very important function; otherwise its accumulation leads to cell aging, malfunction and death [37].

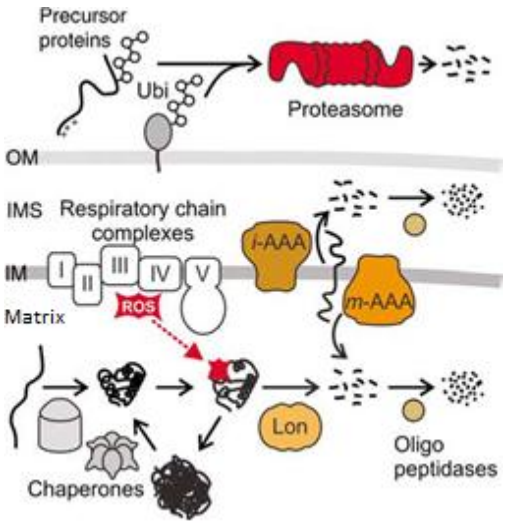

Figure 3: QC applied to mitochondrial proteins. ATP-dependent proteases present in various mitochondrial compartments recognize non-native polypeptides and trigger their proteolysis to peptides that are further degraded by oligopeptidases. At the same time, energy-dependent proteases can act as processing enzymes ensuring assembly and integrity of OXPHOS complexes [31].

QC within mitochondria is, by one side, monitored by nuclear-encoded chaperones, that help proteins achieve their proper tertiary structure, and by other side, by proteases which function is to degrade proteins that fail to fold to properly oligomerize [31] or become damaged [38], where the central role of this last described QC function, belongs to the a superfamily of proteases, the ATPases associated with a variety of cellular activities (AAA^+), which is characterized by a conserved module present in all of these proteases [31]. These proteins are present in each of the four mitochondrial compartments, recognizing misfolded, solvent-exposed domains of substrates, loops of multispanning membrane proteins, or short N- or C-terminal tails protruding from the lipid bilayer [39], having the task to fold and assembly unfolded and misfolded proteins that can accumulate in each of these four compartments (Figure 4) [38].

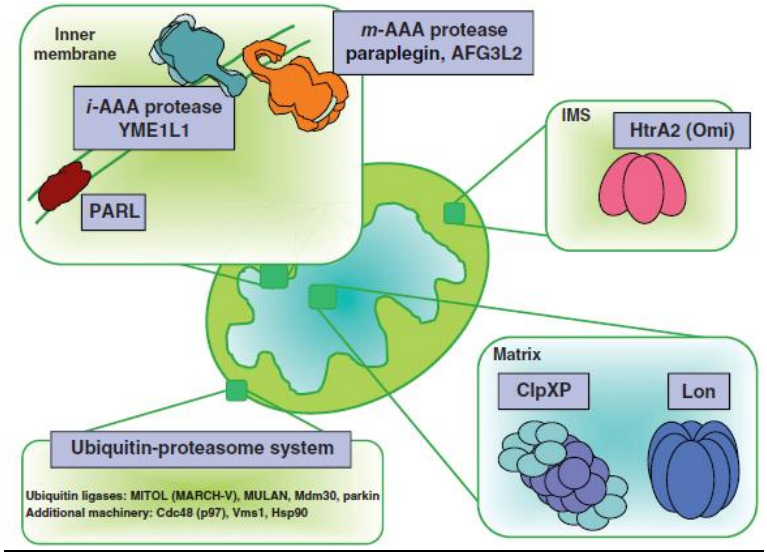

Figure 4: QC proteases monitor the four mitochondrial compartments. Localized QC proteases monitor and protect all four mitochondrial compartments against deleterious accumulation of misfolded, misassembled or unfolded proteins [38].

As observed in Figure 4, in the IM there are two AAA proteins, one with its active site turned to the IMS, the i-AAA, and another one with its active site turned into to the mitochondrial matrix, the m-AAA, being both the prime targets of mitochondrial ROS [31]. Both of these proteases mediate the ATP-dependent dislocation of substrate proteins from the membrane allowing their degradation in a hydrophilic environment [39].

As a member of the QC system [40], m-AAA can be organized in hetero- or homo-oligomeric assemblies [41], being an integral membrane protein, playing a central role in the polypeptides transport through the IM [42]. Within mitochondria, m-AAA proteases have versatile activities, being not only quality control enzymes that completely degrade non-assembled or misfolded polypeptides [40], but can also act as processing enzymes specifically cleaving mitochondrial proteins with regulatory functions, having a chaperone-like activity [33; 41]. In addition to its function in QC, m-AAA proteases control directly the biogenesis of the OXPHOS complexes. As described by Nolden *et al*. [43], MrpL32 is a nuclear encoded subunit of mitochondrial ribosomes, which is matured by m-AAA proteases, having in this case, the role of processing this ribosomal subunit and not of a QC enzyme (Figure 5a). Being MrpL32 processing a prerequisite for its assembly into

ribosomes and activation of mitochondrial translation, the m-AAA protease directly regulates the synthesis of mtDNA-encoded OXPHOS subunits within mitochondria [31]. It is important to note that both regulatory and QC functions of the m-AAA protease are interdependent and may compete with each other, because while m-AAA is degrading its accumulated substrates, resulted from aging and ROS production, this protease will not be assembling MrpL32, resulting in an inhibition of OXPHOS proteins translation [43]. The m-AAA protease is also related to a protective function, regarding OXPHOS complexes, mediating maturation of the ROS scavenger cytochrome c peroxidase (Ccp1) in the mitochondrial intermembrane space, where Ccp1 is processed by the m-AAA protease and the rhomboid protease Pcp1(Figure 5b), an intramembrane-cleaving peptidase in the inner membrane [44].

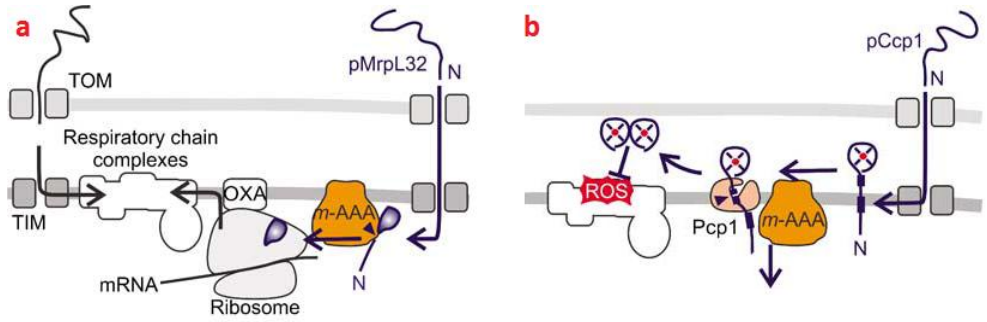

Figure 5: Regulation of OXPHOS complexes assembly and maintenance by proteases. (a) The assembly of mitochondrial ribosomes and synthesis of mitochondrially encoded RC subunits require maturation of newly imported MrpL32 by the m-AAA protease. (b) Biogenesis of the ROS scavenger Ccp1 in yeast mitochondria depends on ATP-dependent membrane dislocation of the precursor protein by the m-AAA protease and maturation by the rhomboid protease Pcp1 [31].

Paraplegin is a subunit of the hetero-oligomeric m-AAA protease, localized in the inner mitochondrial membrane, with the active site in the mitochondrial matrix [45], as shown in Figure 4 and Figure 5. Paraplegin has three domains, where one of them has an AAA^+ module, making paraplegin part of the AAA^+ superfamily [46]. Also, this protein forms cylindrical hetero-hexamers to become active, a known feature from AAA^+ proteins family [47]. The m-AAA protein complex is both responsible for QC in the IM and protein activation [48], and specifically, paraplegin is involved in misfolded proteins degradation, cleavage of mitochondrial targeting sequences, mitochondrial ribosome maturation [43] and is

also linked to the proteolytic processing of OPA1, a GTPase in the IM, which alteration cause optical atrophy [49].

Given the protective functions of mitochondrial QC, it is not surprising that pathological alterations of its key components has been described for an increasing number of neurodegenerative disorders [31], although the involvement of QC system was not yet reported for diabetes mellitus-induced mitochondriopathy.

1.3.1. Regulation of mitochondrial cristae morphology

Mitochondrial cristae and m-AAA proteases depend on each other, since m-AAA exist in mitochondrial cristae, and the cristae need the QC proteins like m-AAA to control the quality of the IM proteins that regulate cristae biogenesis, such as mitofilin [50] and OPA1 [51; 52]

The ultrastructural variations in mitochondria architecture occur mainly due to differences in the amount and shape of the cristae, which derive from the unfolded inner membrane where OXPHOS complexes and intermediate metabolic proteins are embedded. Mitochondria can adapt remarkably well to the energetic needs by altering their metabolism, which is accompanied by structural changes of the inner membrane. For example, abundant cristae are found in mitochondria from tissues where energy demand is high [53]. In the maintenance of mitochondrial cristae organization and the consequent assembly of OXPHOS, other proteins besides QC systems are involved [54]. Mitofilin is an integral membrane protein of the inner mitochondrial membrane, expressed in two isoforms with 88 and 90KDa, that differ in 11 amino acid residues [53; 55], generated through alternative splicing [55]. John *et al.* [53] observed that mitofilin downregulation results in drastic changes in the inner mitochondrial membrane, such as the absence of cristae junctions and the loss cristae traditional structure into concentric layers that interconnect at numerous sites. These authors also observed an increment of IM:OM ratio, suggesting a loss of inner membrane configuration and IM biogenesis, but with a defective OXPHOS, that lead to an increment of membrane potential and a high ROS production, resulting in a weak ATP production. Is this

work, they concluded that mitofilin is an indispensable part of mitochondrial morphogenetic machinery.

1.4. Mitochondrial biogenesis in the striated muscle

The energetic metabolism of skeletal muscle consists mostly in the oxidation of carbohydrates and lipids within mitochondria, being glycogen, the major carbohydrate substrate for ATP production. Rarely, amino acids from protein degradation can be also used as energy source [56]. Also, an anaerobic metabolism is constant within muscle cells, turning glucose into lactate, and only used in higher ratios when a quick and enormous amount of energy is needed [57], even with the high mitochondrial concentration of this tissue [58].

Mitochondrial protein content varies from organ to organ [59], and in striated muscle there is the added dimension of two populations of mitochondria: subsarcolemmal (SS) mitochondria, which exist under the sarcolemma, and intermyofibrillar (IMF) mitochondria, which exist trapped into the myofibrils [60; 61; 62]. Several studies reported that the two mitochondrial subpopulations have different and specific roles in producing ATP for the cell [19; 20; 22]. For instance, IMF mitochondria are involved in the production of energy for contractile activity, whereas SS mitochondria provide energy for membrane and transport functions (Figure 6) [20]. Also, the metabolic differences between these mitochondrial subpopulations may play an important role with functional and physiological consequences [63].

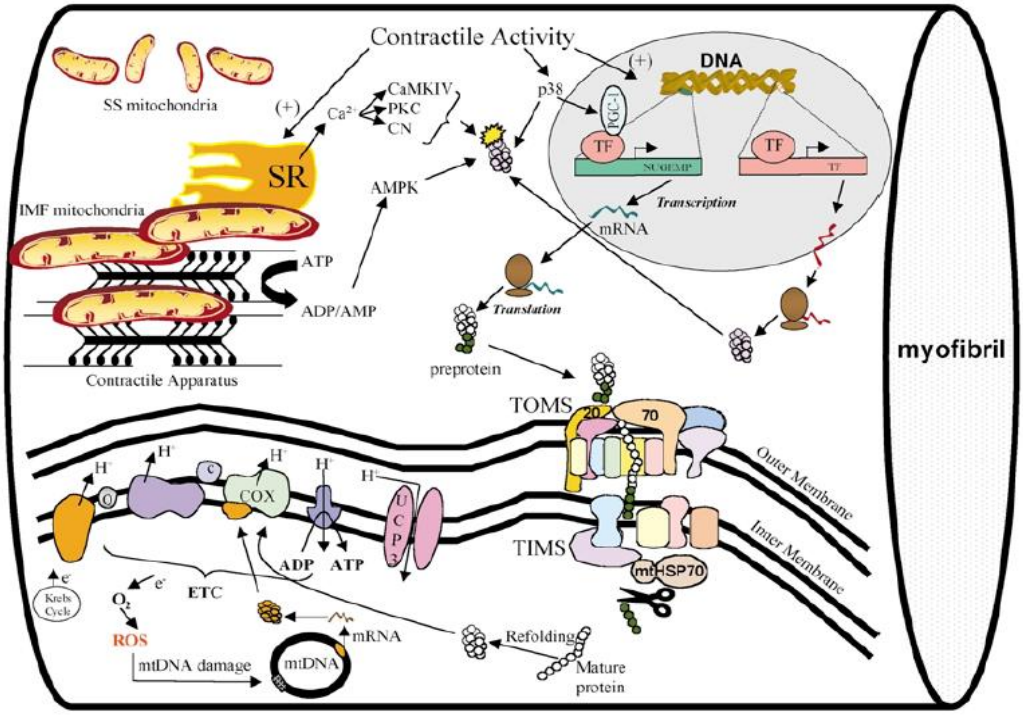

Figure 6: Contractile activity-induced molecular adaptations within skeletal muscle which lead to IMF and SS mitochondrial biogenesis and the expression of nuclear genes encoding mitochondrial proteins (NUGEMPs) [64].

According to Riva *et al*. [65], these SS and IMF subpopulations have also different cristae morphology and structure, with SS mitochondria presenting predominantly lamelliform cristae, while IMF has both lamellar and tubular shaped cristae (Figure 7) [22; 65].

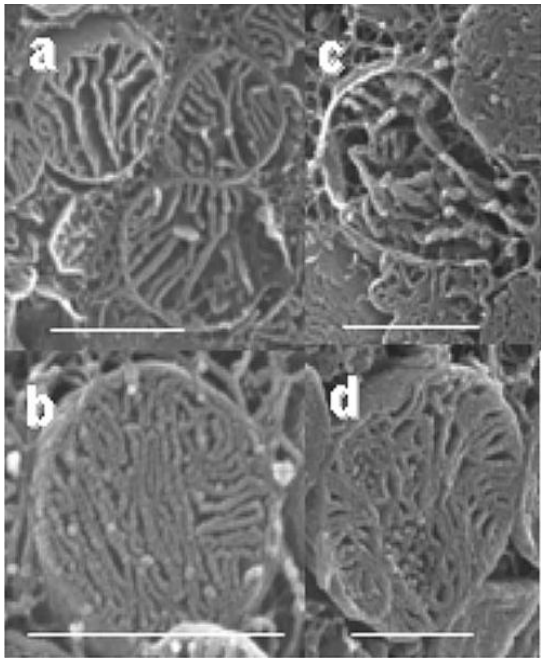

Figure 7: Osmium-extracted mitochondria. Strands in background are ribbons of agarose. (a): Cluster of SS with solely lamelliform cristae. Scale bar, 1µm. (b): SS with mostly lamelliform cristae. Scale bar, 0.5µm. (c): IMF with exclusevely tubular cristae. Scale bar, 0.5 µm. (d): IMF with mainly lamelliform cristae. Scale bar, 0.5µm [65].

Each of these subpopulations also has different capacities for protein synthesis, biochemical functionality and mitochondrial respiration [63]. They present different lipid and protein compositions, giving them different densities [60; 61; 62]. Some studies suggested the involvement of different regulatory mechanisms for mitochondrial biogenesis under different stimuli, suggesting that these mitochondrial subpopulations have a different role in the cell's economy [20; 22; 61; 64].

In the work of Kuznetsov *et al.* [63], it was shown that SS mitochondria exist densely packed under the sarcolemma (Figure 8) and seem to have a shielding function against ROS, protecting the cell from the high oxygen concentrations, suggestive of a higher oxidized state of SS mitochondria compared to IMF [66].

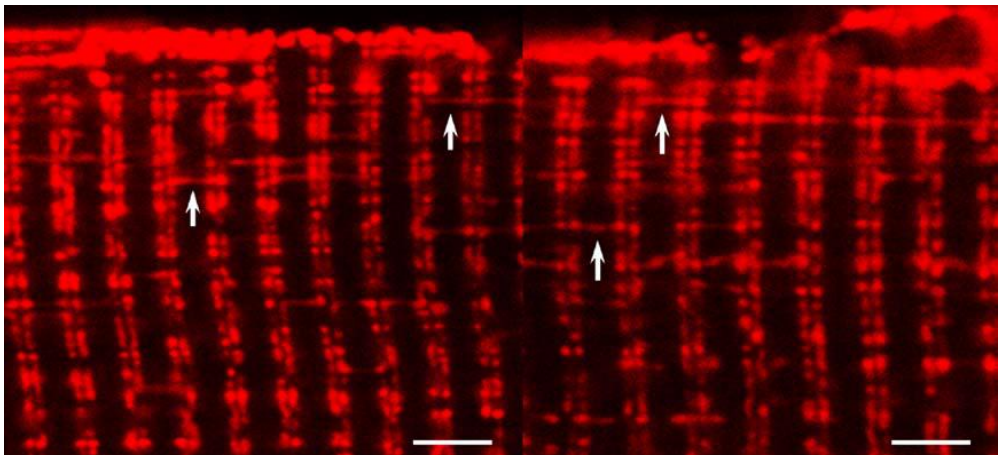

Figure 8: Organization of SS mitochondrial clusters in rat *soleus* muscle. Clusters of subsarcolemmal mitochondria are densely packed. Mitochondria located near the outer cell membrane demonstrate interconnections and mitochondrial network (arrows), whose are necessary to synchronize mitochondrial activities between contractions cycles and to share the metabolic feedback regulation of mitochondrial respiration via energy transfer networks. *Soleus* mitochondria were labeled with Rhod-2. Scale bars, 5 μm [63].

Hood *et al.* [67] also described SS mitochondria as more unstable than the IMF subpopulation, making them more plastic to distinct stimuli as chronic muscle use or disuse and pathological conditions.

1.5. Mitochondrial impairment in type 1 diabetes *mellitus*

T1DM, also called juvenile or insulin-dependent diabetes, is a chronic and metabolic disease characterized by the autoimmune process targeting the β-cells in the islets of Langerhans, causing their destruction and dysfunction, diminishing the production of insulin, which allows the transport of glucose from the blood to the cells, resulting in an abnormal high level of glucose in blood and a deficiency of glucose within cells [2]. Glucose, as the main energy source of the organism, is necessary for cells functions, but when in low concentrations, it brings several complications to the normal performance of cells and tissues in the organism. Skeletal muscle is an extremely energy demanding tissue, highly reliant on mitochondrial oxidative metabolism, being its impairment associated with diabetic dysfunction [68]. Several studies suggest that hyperglycaemia leads to oxidative damage of muscle mitochondria, intrinsically associated with increased ROS production [69]. Being the most relevant cell source of ROS, mitochondria are at

the same time targets of its own ROS generation. Mitochondrial proteins and mtDNA are particularly prone to oxidative damage [70; 71]. These misfolded proteins lead to OXPHOS dysfunction, increasing ROS production that will damage more mitochondrial proteins, creating a vicious cycle of misfolded protein and ROS production, as represented in Figure 9. The accumulation of misfolded proteins within mitochondria will activate the mitochondrial upregulation response (UPR^{mt}), increasing QC proteins, in order to balance the homeostasis [38]. This phenomenon was observed in various aging diseases.

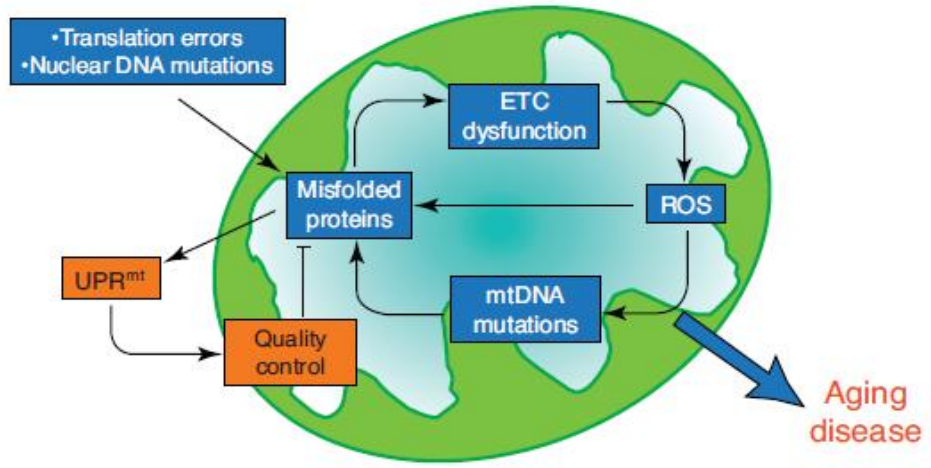

Figure 9: Relationship between mitochondrial protein folding, metabolism and dysfunction. Mitochondrial protein homeostasis depend upon a balance between deleterious aspects of cellular and organelle biology that can produce large amounts of misfolded proteins (blue boxes) and the protective mechanisms such as the QC machinery and the mitochondrial upregulation (UPR^{mt}), that protect against the accumulation of misfolded or damaged proteins (orange boxes) [38].

In several studies, type 1 diabetes-induced mitochondrial alterations were observed at a morphological level, through microscopic techniques directly [62]. T1DM mitochondria have less density [72], show less cristae [73; 74], are in decreased number in liver and heart [74; 75], have an increased sectional area, observed using transmission electron microscopy [76], possibly resulted from mitochondrial swelling [74; 76]. These alterations are possibly related with the impairment of QC proteins and other mitochondrial proteins, making their study important for a better understanding of the molecular mechanisms underlying T1DM and its complications.

1.6. Objectives

In order to get a deep insight into the molecular mechanisms underlying type 1 diabetes complications-induced mitochondriopathy in skeletal muscle, the general aim of our work was to study the regulatory role of proteolysis in OXPHOS organization and functionality in pure fractions of SS and IMF mitochondria isolated from *gastrocnemius* muscle of STZ-induced diabetic rats. In this sense, mitochondria morphology, respiratory chain complexes organization and functionality, proteolytic activity and the expression of specific proteins such as paraplegin, mitofilin and ATP synthase β was evaluated.

2. Material and Methods

2.1. Animals

The experimental protocol was performed using 20 Wistar male rats (*Rattus norvegicus*), 8 weeks old and weighting 200g, at the beginning of the experiments. The animals were randomly divided into two groups (n=10 per group): a control group, and a T1DM group. In order to induced T1DM, rats from the group with T1DM were injected intraperitoneally with a single injection of 60mg/Kg of streptozotocin (STZ) diluted in sodium citrate buffer (pH 4.5) [77] and the control group of rats were injected with the same volume of sodium citrate buffer. Twenty-four hours after the STZ administration, the glycemia was evaluated and the animals were considered diabetic when the levels of blood glucose were higher than 250mg/dL. During the experimental protocol, animals were housed in collective cages (2-3 rats per cage) and were maintained in a room at normal environment (21–22 °C; ~50–60% humidity) receiving food and water *ad libitum* in 12h light/dark cycles. After 4 months of STZ administration, the glycemia and was measured and the animals were sacrificed through cervical dislocation, and the *gastrocnemius* muscles were extracted for mitochondrial extraction. Pools of muscles from 3 or 4 rats (n=3) were performed.

The experimental protocol followed the specifications and recommendations from the "Guide for Care and Use of Laboratory Animal" from the Institute for Laboratory Animal Research (ILAR 1996).

2.2. Isolation of SS and IMF mitochondrial subpopulations

Mitochondrial populations were isolated from the *gastrocnemius* muscle following the protocol described by Ferreira *et al.* [62]. All the procedures were performed on ice or below 4ºC. Muscle tissue was washed three times with extraction buffer (EB) (20mM 3-(N-morpholino)propanesulfonic acid (MOPS), 110mM KCl, 1mM ethylene glycol-bis(2-aminoethylether)-*N*,*N*,*N′*,*N′*-tetraacetic acid (EGTA), pH 7.5). The tissue, after being minced with scissors, was incubated

in EB with 0.25mg/mL trypsin (Promega, Wisconsin, USA), during 25min on ice. Buffer was then replaced by EB with 10mg/mL of albumin fat-free (Sigma). The tissue was washed with EB and homogenized with a Potter homogenizer (Teflon pestle). Large cellular debris and nuclei were pelleted by centrifugation for 5min at 1000xg. The resulting supernatant was centrifuged for 20min at 16000xg and the pellet was gently re-suspended in a small volume of sucrose buffer (SB) (250mM sucrose, 0.1mM EGTA, 10mM Tris-HCl, pH 7.4), to a final protein concentration of 8–15mg/mL and further purified on a density-gradient with 50% v/v Percoll (Sigma). After centrifugation at 95000xg for 30min, two mitochondrial subpopulations were obtained; a lower brown band, corresponding to IMF mitochondria, and an upper one consisting of SS mitochondria. The mitochondrial subpopulations were washed twice with SB and after final purification were aliquoted for electron microscopic analysis, BN-PAGE, respiratory chain complexes IV and V in-gel activity assays, zymography and western blot analysis. Protein content was determined with RC DC Protein Assay kit (Bio-Rad, Hercules, CA, USA) and DNA content was quantified with QubitTM fluorometer (Invitrogen, Carlsbad, CA, USA).

2.3. Electron microscopic analysis and average mitochondrial area calculation

For morphological characterization, 75µL of mitochondrial suspension of each subpopulation from both groups were centrifuged at 7000xg for 10 minutes and the resulting pellet was fixed with 2.5% gluteraldehyde, postfixed with 2% osmium tetroxide, dehydrated in graded ethanol and embedded in Epon. Ultra-thin (100nm) sections from mitochondrial suspensions were contrasted with uranyl acetate and lead citrate for TEM (transmission electron microscopy) analysis (Zeiss EM 10A). For mitochondria morphometric evaluation, photographs of ultrathin sections were digitalized and analyzed with the NIH Image J (Image Processing and Analysis in Java, USA) software. In each experiment, more than 150 mitochondria from SS and 800 mitochondria from IMF subpopulation suspension were analysed for organelle sectional area quantification.

2.4. BN-PAGE and in-gel activity of OXPHOS complexes IV and V

BN-PAGE was performed using the method described by Schagger and von Jagow [78] with minor modifications. Mitochondria (200 μg of total protein), from each mitochondrial subpopulation (duplicate of n=3), were pelleted by centrifugation at 20000xg for 10min and ressuspended with the solubilization buffer (50mM NaCl, 50mM Imidazole, 2mM ε-amino n-caproic acid, 1mM EDTA, pH 7.0) with 1% w/v digitonin. After 10min on ice, insoluble material was removed by centrifugation at 20000xg for 20min at 4ºC. Soluble components were combined with 0.5% w/v Coomassie Blue G250, 50mM ε-amino n-caproic acid, 4% w/v glycerol and separated on a 4–13% acrylamide gradient gel with 3.5% sample gel on top. Gels were run in a SE600 Electrophoresis Unit (Hoefer). Anode buffer (25mM Imidazole, pH 7.0) and cathode buffer (50mM tricine and 7.5mM Imidazole, pH 7.0) containing 0.02% w/v Coomassie Blue G250 was used during 1h at 70V, the time needed for the dye front reach approximately one-third of the gel. Cathode buffer was then exchange for one with 0.002% w/v Coomassie Blue G250 and the native complexes were separated at 200V for 3h at 4ºC. Native standard markers (GE Healthcare) were used. The gels were stained with 0.12% w/v Coomassie Blue G250 prepared in 20% methanol, after 1 h fixation in a solution of 10% acetic acid and 40% methanol. Gels were then destained with 25% methanol and scanned with Gel Doc XR System (Bio-Rad).

The in-gel activity and histochemical staining assays of complexes IV and V were determined using the methods described by Zerbetto *et al.* [79] with minor modifications. After the membrane complexes separation through BN-PAGE, complex IV-specific heme stain was determined using 10μL horse heart cytochrome c (5mM) and 0.5mg diaminobenzidine dissolved in 1mL 50mM sodium phosphate, pH 7.2. The reaction was stopped by 50% v/v methanol and 10% v/v acetic acid, and the gels were then transferred to water. ATP hydrolysis activity of complex V was analyzed by incubating the BN-PAGE gels with 35mM Tris, 270mM glycine buffer, pH 8.3, at 37ºC, which had been supplemented with 14mM $MgSO_4$, 0.2% w/v $Pb(NO_3)_2$ and 8mM ATP. Lead phosphate precipitation that is proportional to the enzymatic ATP hydrolysis activity was stopped by 50%

v/v methanol (30min), and the gels were then transferred to water. Band detection, quantification and matching were performed using QuantityOne® Imaging software (v4.6.3, Bio-Rad) as a function of density (intensity/mm^2). The Volume Rectangle Tool was used to measure the total signal intensity inside a boundary drawn around the bands. Background was subtracted from each band volume by using local background subtraction. Intensities of bands acquired from each protein extract were compared and results were expressed as arbitrary units of optical density (OD).

2.5. Protease activity analysis through gelatin zymography

The zymographies were performed using a 10% SDS-PAGE separation gel with 0.1% of gelatin (n= 3). 40µg of each sample was incubated on charging buffer (100mM Tris pH 6.8, 5% SDS, 20% glycerol, 0.1% bromophenol blue) for 10 minutes on ice, in a proportion of 1:1 (v/v). After separation, the gels were incubated in renaturation buffer (2.5% Triton X-100) for 30 minutes, with soft agitation. Then, the zymogram gels were changed to a development buffer (50mM Tris, 5mM NaCl, 10mM $CaCl_2$, 1µm $ZnCl_2$, 0.02% (v/v) Triton X-100, pH 7.4) for more 30 minutes, also with soft agitation. Finally, the gels were changed to a new development buffer, and incubated overnight at 37ºC.

The zymography gels were stained with 0.12% w/v Coomassie Blue G250 prepared in 20% methanol, after 1 hour fixation in a solution of 10% acetic acid and 40% methanol. Gels were then destained with 25% methanol and scanned with Gel Doc XR System (Bio-Rad).

2.6. Proteases identification from zymography and SDS-PAGE gels

The zymography bands with proteolytic activity and the correspondent bands from the SDS gel were excised. The bands from the zymography were washed four times with 25mM of ammonium bicarbonate/ 50% acetonitrile, while the bands from the SDS were washed just two times. The dehydration of the bands

was performed with a final wash with 100% acetonitrile, followed by a drying in a SpeedVac® Plus SC 210 A (Thermo Savant, USA). After dried, it was added 20µL of Trypsin (Catalogue #V511A, Promega Corporation, USA) in ammonium bicarbonate 25mM (concentration of Trypsin of 10µg/mL), and incubated for 1 hour at 37ºC, in order to the gel absorb the maximum possible Trypsin, then 30µL of more ammonium bicarbonate 25mM was added, and a new incubation was performed overnight also at 37ºC. The digested peptides were extracted from the gel with 10% formic acid and concentrated under vacuum in the SpeedVac® Plus SC 210 A (Thermo Savant, USA). Finally, the peptides were ressuspended in 10µL of 50% acetonitrile/ 0.1% formic acid solution, centrifuged for 5 minutes at 15000rpm and transferred to a HPLC vial for peptide separation.

The peptide separation through HPLC was performed in the separation module Ultimate 3000 (LC Pachings), using a capillary column (C18 Zorbax SB 300; 0.75µm of internal diameter; 15cm length). A gradient was used from the A solvent – H_2O/ acetonitrile/ trifluoracetic acid (95:5:0.05 v/v/v) – to the B solvent – H_2O/ acetonitrile/ trifluoracetic acid (20/ 80/ 0.04 v/v/v). For the separation 2µg/µL of sample were injected. The separation was performed using a linear gradient (5-55% B solution, for 30 minutes, 55-80% B solution for 10 minutes and 80-5% A solution for 5 minutes), each one with a flow of 0.3µL/min. After being eluted from the column, the peptides were directly applied into a MALDI plaque in 20 seconds fractions, using an automatic collector (LcPackings), with the addition of 270nL of α-ciano-4-hidroxicinâmic acid matrix (6mg/mL of α-ciano-4-hidroxicinâmic acid matrix prepared in 70% acetonitrile and 0.3 trifluoracetic acid, supplemented with 0.4µL of a Glu-Fib solution (15fmol)) for later identification of the proteases detected through zymography.

The mass spectra of the peptides resulted from the proteins tryptic digestion and HPLC separation, were obtained with a mass spectrometer MALDI-TOF/TOF (4800 Proteomics Analyzer, Applied Biosystems, Foster City, CA, USA), in positive reflectron mode and obtained in the mass interval between 700 and 4500Da, with 1000 laser shots. It was created a data acquisition method to select the 10 most intense peaks in each spot for later MS/MS specter acquisition, excluding the matrix peaks due trypsin or acrylamide autolysis. The internal

standard Glu-Fib peak (m/z1570.68Da) was used as internal calibrating of the equipment. The spectra were processed and analyzed by Global Protein Server (GPS) Workstation (Applied Biosystems), which uses as search engine the Mascot (Matrix Science, London, UK), for protein identification conjugated with the data of PMF (peptide mass fingerprinting), with the data of MS/MS for internal data base search. The protein identification was accepted when the confidence degree was bigger than 99%.

2.7. Western Blot analysis

Equal amounts of proteins from each mitochondrial population (duplicate of n=3) were electrophoresed on a 10% SDS-PAGE gel, followed by blotting on a nitrocellulose membrane (Hybond-ECL; Amersham Pharmacia Biotech, Buckinghamshire, UK). After blotting, non-specific binding was blocked with 5% w/v nonfat dry milk in TTBS (TBS ((tris-buffered saline) 100mM Tris, 1.5mM NaCl, pH 8.0) with 0.5% Tween-20) and the membrane was incubated with primary antibody (anti-paraplegin (H-180: sc-135026 Santa Cruz Biotechnology, INC. (CA, USA), anti-ATP synthase (cat. no. ab14730 Abcam (Cambridge, UK) or anti-mitofilin (cat. no. ab48139 Abcam (Cambridge, UK)), diluted 1:1000 in 5% w/v nonfat dry milk in TTBS for 2 h at room temperature, washed and incubated with secondary horseradish peroxidase-conjugated anti-mouse or anti-rabbit (GE Healthcare), respectively. The blots were developed by using enhanced chemiluminescence detection system (Amersham Pharmacia Biotech) according to the manufacturer's instructions, followed by exposure to X-ray films (Sigma, Kodak Biomax Light Film, St. Louis, MO, USA). The protein bands on films were visualized using a GelDoc XR (Bio-Rad) and quantified by QuantityOne® imaging software (v4.6.3, Bio-Rad) as explained above.

2.8. Statistical analysis

The optical densities of each protein band in BN-PAGE and zymograhy gels were exported, after normalization, from QuantityOne® imaging software (v4.6.3,

Biorad), to GraphPad Prism 5, were the unpaired Student's t-test was performed, using a 95% confidence degree, in order to evaluate the expressed differences between the two group (control and diabetic).

3. Results

3.1. Validation of the experimental T1DM animal model

In this study we used an animal model obtained by intraperitoneal administration of a single dose of 60mg/Kg streptozotocin (STZ). In order to validate the animal model, glycemia and glycated hemoglobin (HbA1c) were evaluated (Table 2).

Table 2: Glicemia and HbA1c measured values for each group (control and type 1 diabetes). The values are presented with mean ± standard deviation.

	Glicemia (mg/dL)	HbA1c (%)
CONT	66.3 ± 15.0	3.96 ± 0.80
T1DM	577.1 ± 234.0***	6.28 ± 1.12***

***p<0.0001 vs. Control

As can be observed in table 1, the rats from T1DM group showed a significantly higher concentration of blood glucose and glycated hemoglobin than the ones from the control group.

The effect of STZ administration was also evaluated in terms of animals' body weight and muscle mass (Table 3).

Table 3: The effect of T1DM in rat body weight, *gastrocnemius* muscle mass and *gastrocnemius* muscle/ body weight ratio. The values are presented with mean ± standard deviation.

	Body weight (g)	**Muscle weight (g)**	**Muscle weight/body weight ratio (mg/g)**
CONT	437.1 ± 58.4	5.69 ± 0.04	13.03 ± 0.001
T1DM	251.0 ± 43.1***	3.99 ± 0.88**	15.90 ± 0.006

****p*<0.0001 vs. Control

As can be seen in table 2, muscle mass significantly decreased (29.9%) in T1DM rats, associated with a lower body weight (42.6%). So, the muscle mass/ body weight ratio presented no differences between the two groups of rats.

The comparison of glycemia, Hb1Ac, muscle mass and body weight values between CONT and T1DM groups clearly evidence a diabetic status of T1DM rats.

3.2. Evaluation of mtDNA and mitochondrial protein concentrations in skeletal muscle

The levels of mtDNA and mitochondrial protein were quantified in IMF and SS mitochondria isolated from *gastrocnemius* muscle. The ratios protein/mtDNA concentrations, mtDNA content/muscle mass and protein/muscle mass were then determined (Table 4). The mtDNA concentration in the muscle was evaluated in order to obtain a rough value of the mitochondrial quantity in the muscle, with which values, was possible to calculate the percentage of each mitochondrial subpopulation in the muscle (Table 4).

Table 4 Effects of T1DM in mitochondrial protein content-to-mtDNA concentration, mtDNA-to-muscle mass and protein content-to-muscle mass. The results are expressed as mean ± standard deviation.

Experimental Group		[Protein]/[mtDNA] ratio ($\mu g.mg^{-1}$)	$mtDNA/m_{muscle}$ ($\mu g.g^{-1}$)	$Protein/m_{muscle}$ ($mg.g^{-1}$)
CONT	**SS**	0.80 ± 0.454	0.11 ± 0.022	0.10 ± 0.069
	IMF	0.52 ± 0.318	0.48 ± 0.034	0.25 ± 0.044
T1DM	**SS**	0.56 ± 0.023	0.37 ± 0.014***	0.21 ± 0.015*
	IMF	0.66 ± 0.079	0.54 ± 0.160	0.35 ± 0.117

***p <0.0001 vs. Control SS; *p <0.05 vs. Control SS**

For both experimental groups, Table 4 shows no significant differences in the mitochondrial protein/mtDNA ratio. A tendency is noticed in control SS to be higher than the samples from diabetic SS, though with no statistical significance.

A significantly higher concentration of mtDNA/muscle mass was noticed in the SS subpopulation of T1DM compared to CONT. No differences were observed among IMF mitochondria from both groups.

For both mitochondrial subpopulations, it was noticed a tendency for higher mitochondrial protein concentration in the muscles from diabetic rats, comparing with control ones. However, the only significant differences were observed for SS mitochondria (p value < 0.05) (Table 4).

3.3. Morphological characterization of mitochondrial subpopulations

In the mitochondria isolation procedure, after the final centrifugation in the Percoll gradient, two different mitochondrial subpopulations with different densities were obtained, corresponding to the two different brown bands observed (Figure 10). The upper band contains SS mitochondria and the lower band contains IMF mitochondria.

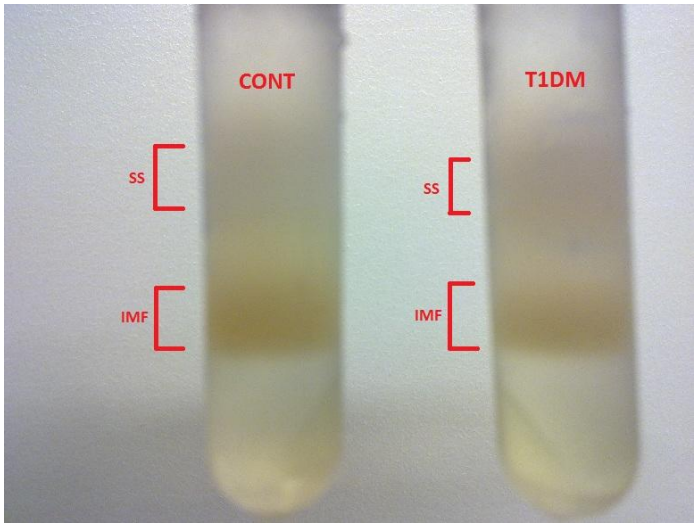

Figure 10: Percoll gradient loaded with crude mitochondrial after ultracentrifugation. Density differences are evident between SS and IMF subpopulations, for both groups in study (CONT and T1DM). No visible differences are noticed between mitochondria from control and T1DM groups.

Once removed from the Percoll, mitochondrial subpopulations were morphologically analysed by transmission electron microscopy (TEM). A general analysis of TEM images of SS populations showed a lot of membranes and few

mitochondria (Figure 11a and b); on the other hand, mitochondria with different shapes and sizes were noticed and no fragmented membranes or any kind of debris was seen in the IMF images (Figure 11c and d).

The micrographs obtained were also used to calculate the mitochondria area (Figure 11e).

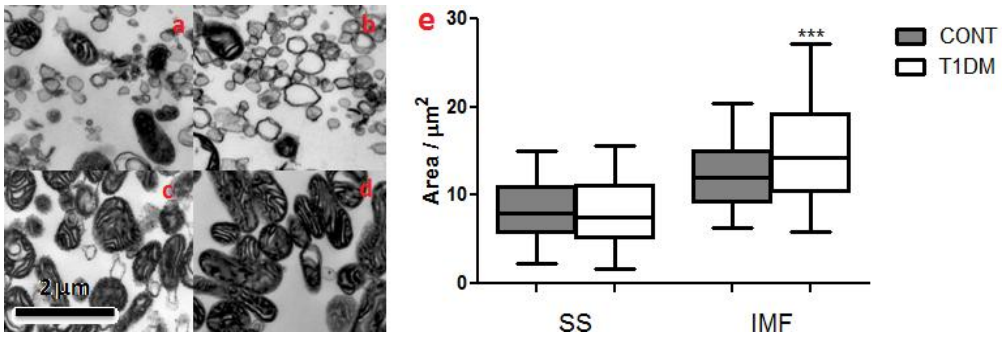

Figure 11: TEM images from: (a) SS mitochondria from control rats, (b) SS mitochondria from T1DM rats, (c) IMF mitochondria from control rats and (d) IMF mitochondria from T1DM rats, with a magnification of 10,000x. (e) Box and whiskers graph where the mitochondrial area of the different populations is compared (n=180 for SS and n=800 for IMF). Scale bar = 2 µm.
******p* < 0.0001 vs. C IMF**

Regarding the average area of each mitochondrial subpopulation in the different groups of rats, no significant difference between SS mitochondrial from control and diabetic rats ($8.401 \pm 0.2413 \mu m^2$ and $8.092 \pm 0.3122 \mu m^2$, respectively) were observed; on the other hand, the statistical analysis evidenced a large difference in size between IMF mitochondria of control and T1DM groups, with smaller mitochondria observed in control rats than in T1DM ($12.22 \pm 0.1321 \mu m^2$ to $14.89 \pm 0.1915 \mu m^2$, p value < 0.0001).

3.4. BN-PAGE and in gel activity of OXPHOS complexes IV and V

In order to evaluate the effect of STZ administration on mitochondrial respiratory chain complexes organization, BN-PAGE analysis of mitochondrial subpopulations was performed. The representative BN-PAGE (Figure 12), show a hauling effect in both lanes with the SS samples (Figure 12a and b), confirmed by the wide peaks in the darker lanes on the right of Figure 12. No qualitative or

quantitative differences of the overall band pattern were observed among isolated IMF mitochondria from both groups of study (Figure 12c and d).

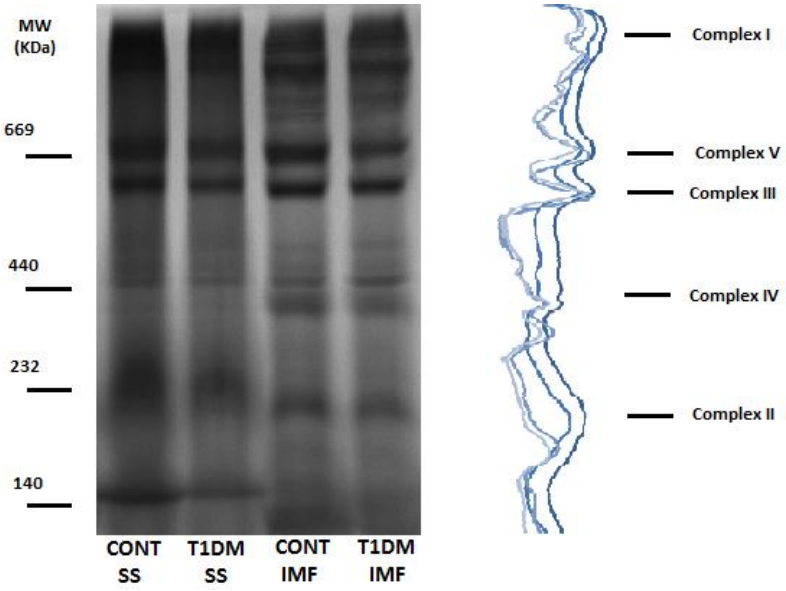

Figure 12: BN-PAGE profile of SS and IMF mitochondria. An overlap of the density variation of the four lanes is presented on the right.

Regarding BN-PAGE separation of mitochondrial respiratory chain complexes (Figure 12), no differences were seen between CONT and T1DM groups for SS or IMF subpopulation. However, comparing SS with IMF mitochondria a slightly different profile was observed suggestive of a different organization of OXPHOS complexes.

In order to evaluate OXPHOS functionality, the in-gel activity of complexes IV and V was determined. The in-gel activity of the CIV showed no quantitative differences between T1DM and controls, in both mitochondrial subpopulations, as can be observed in Figure 13a.

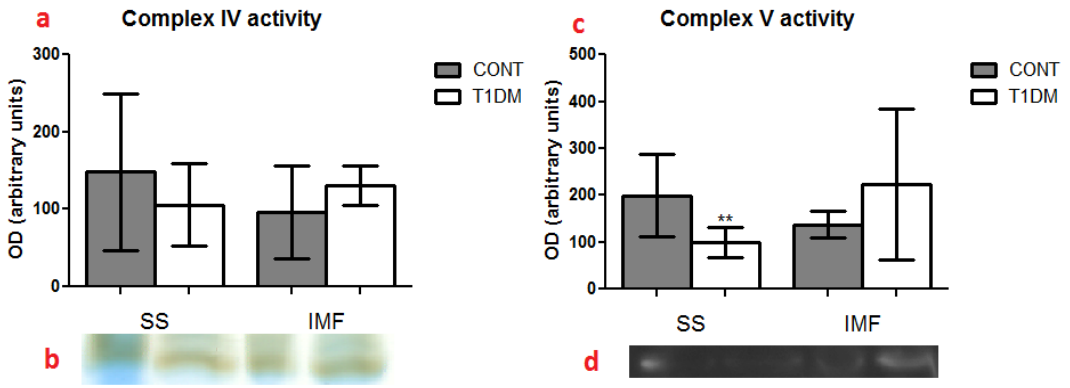

Figure 13: Effects of T1DM in the in-gel activity of respiratory chain complexes IV (a) and V (c) of mitochondrial subpopulations SS and IMF, with respective representative images (b+d). The OD results are expressed in arbitrary units (mean ± standard deviation).
****p* < 0.01 vs. Control SS**

Regarding CV, significant differences were only observed within SS subpopulation, with T1DM presenting lower activity than control groups (Figure 13b).

3.5. Gelatin zymography analysis

The global analysis of mitochondrial proteolytic activity was performed by gelatin zymography. Two light bands were observed for each sample: one poorly visible upper band, with around 25KDa, and a more visible at a lower position in the gel, with around 15KDa (Figure 14a). These bands were extracted from zymography and corresponding SDS-PAGE gels and analysed by nLC-MS/MS for proteases identification. Nevertheless, no positive identifications were achieved due to technical problems.

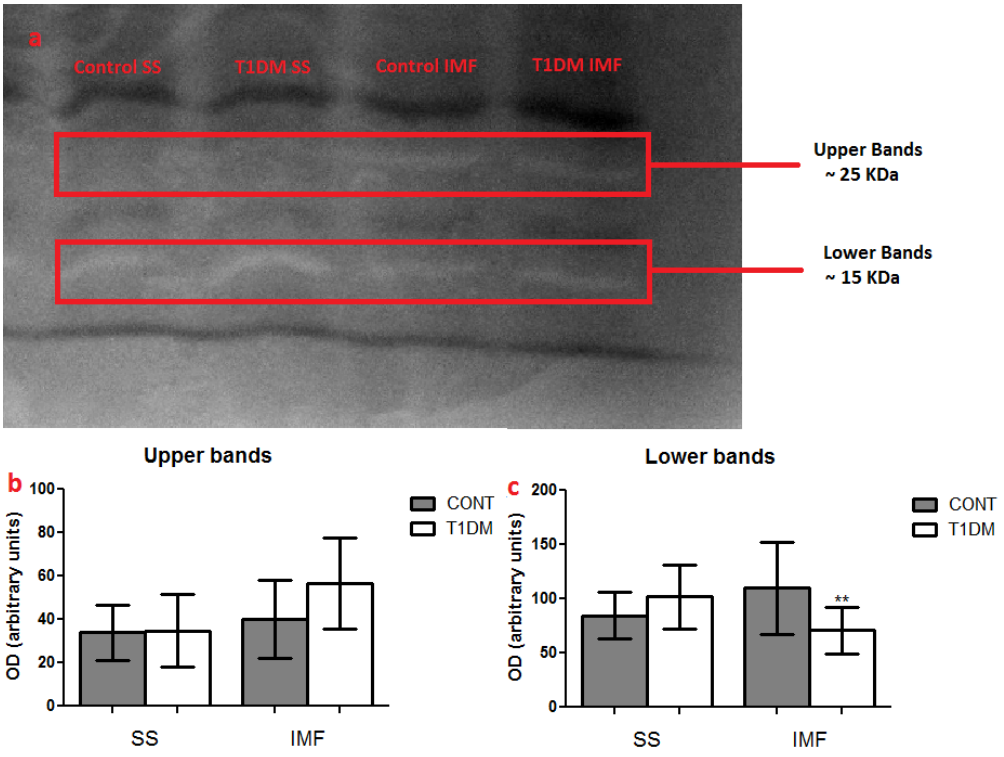

Figure 14: Effects of T1DM in the proteolytic activity of mitochondrial subpopulations (SS and IMF) (a) Representative image of the zymography evidencing two light bands with noticeable proteolytic activity. Comparison of OD variation for each band: the upper band (b) and the lower band (c). The OD results are expressed in arbitrary units (mean ± standard deviation).
****p* < 0.01 vs. Control IMF**

The analysis of OD variation among different subpopulations and groups was performed for each band with proteolytic activity. No differences were noticeable between both control and diabetic groups in the upper band, for both mitochondrial subpopulations (Figure 14b). On the other hand, for IMF mitochondria was visible a higher activity in the control group regarding the lower band (Figure 14c).

3.6. Western blot analysis

The expression of several proteins (ATP synthase subunit β, paraplegin and mitofilin) was evaluated by western blotting. Regarding ATP synthase subunit β, no differences between CONT and T1DM groups were observed, for both mitochondrial subpopulations (Figure 15).

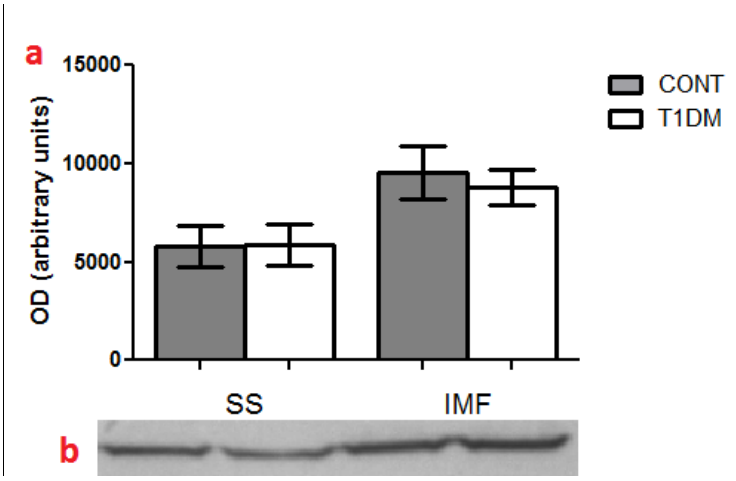

Figure 15: (a) Effects of T1DM in the ATP synthase expression in the different mitochondrial subpopulations. The OD results are expressed in arbitrary units (mean ± standard deviation). (b) Representative image of the Western blot.

The paraplegin analysis showed a different tendency between the two mitochondrial subpopulations (Figure 16), with higher OD values observed in T1DM group regarding SS subpopulation. In opposition, higher expression levels of this protease were noticed in the control group of IMF mitochondria, when compared to T1DM group (p value < 0.0001).

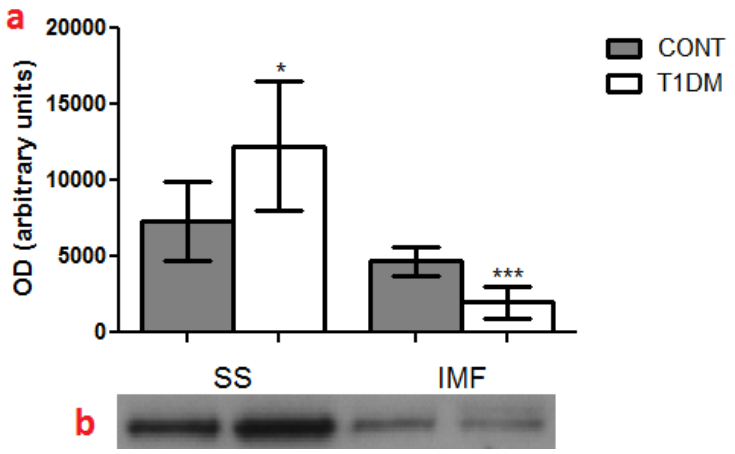

Figure 16: Effects of T1DM in paraplegin expression in the different mitochondrial subpopulations (SS and IMF). The OD results are expressed in arbitrary units (mean ± standard deviation). (b) Representative image of the Western blot.

***p< 0.05 vs. Control SS; ****p* < 0.0001 vs. Control IMF**

The mitofilin analysis evidenced two very distinct bands in IMF samples, corresponding to the two mitofilin isoforms (Figure 17). No signal was detected in

the immunoblots for SS mitochondrial samples. Only one OD value was considered in the analysis of mitofilin expression, corresponding to the sum of both bands' OD (Figure 17).

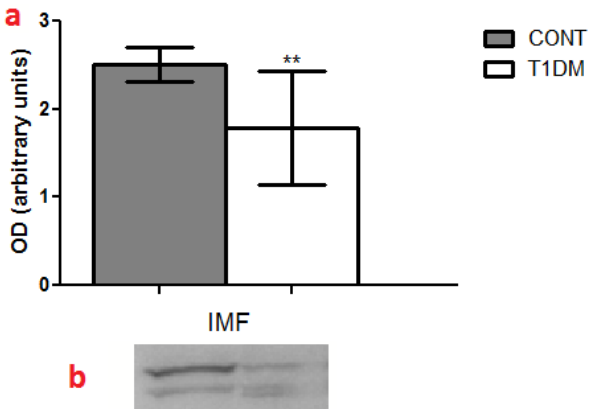

Figure 17: Effects of T1DM in mitofilin expression, in IMF mitochondrial subpopulation,. The OD results are expressed in arbitrary units (mean ± standard deviation). (b) Representative image of the Western blot.
****p* < 0.01 vs. Control IMF**

The control group showed significantly higher expression levels of mitofilin (*p* value < 0.01) than T1DM (40.9%).

In a general overview, in the *gastrocnemius* from T1DM rats, IMF mitochondria presented the higher alterations, whereas SS mitochondria suffered minor alterations, with paraplegin upregulation and increased mitochondrial biogenesis, regarding mtDNA-to-muscle mass as a rough measure of mitochondrial concentration, showing a better adaptation of this subpopulation to type 1 diabetes than IMF mitochondria.

4. Discussion

Diabetes *mellitus* has been described in several studies as the epidemy of XXI century [80; 81; 82]. The study of Shaw *et al*. [1], report that the incidence of diabetes *mellitus* has increased, and in 2010 affected 285 million people worldwide, with a tendency to increase to 439 million people until 2030. T1DM is the less studied type of diabetes *mellitus*, but it is urgent to better understand this disease, since it has an autoimmune origin and the patients have low life quality due to the complications that arise very early in their life.

In order to mimic T1DM and its complications, Wistar rats were injected with a single dose of STZ (60mg/Kg). Streptozotocin (STZ) specifically attacks β cells, because it has a glucose-similar structure, which allows its recognition by Glut-2 transporters, being able to reach the cell nucleus, where this drug acts by destroying the cellular genome [83]. The high glycemia and HbA1c levels measured in the rats from the group with T1DM, together with the notorious polyuria and polydipsia presented by these animals during the experimental protocol, proved that STZ administration successfully induced T1DM (Table 2). These results were also supported by the observed muscle weight loss, and consequent body weight loss in the rats from the T1DM group (Table 3), in a similar way as previously reported [84; 85]. The unaltered muscle weight/ body weight ratio showed that body weight loss, in the rats with T1DM, was a consequence of muscle weight loss, in these animals.

In order to evaluate if these phenotypic alterations were related with mitochondrial morphological and biochemical changes, the two mitochondria subpopulations were studied. The differences between the IMF mitochondria sectional areas were significant, with mitochondria from the T1DM group presenting higher values than the ones from the control group (Figure 11). These results are in accordance with the previously reported by Cester *et al.* [76], that noticed a T1DM-related mitochondrial volume increment, possibly a mitochondrial response to impaired respiration through the increase of the ratio surface area-to-volume [86]. These changes in the IM might be related with mitofilin

underexpression (Figure 17), since this protein is responsible for cristae assembly [53], as well as paraplegin underexpression (Figure 16), a protease involved in OPA1 maturation, a dependent cristae morphogenesis within mitochondria, by keeping its cristae junctions [87].

In the *gastrocnemius* muscle from the control group, the measured percentage of each population is the same as described in literature [60], considering mtDNA-to-muscle mass content, with SS mitochondria corresponding to 19% of the total mitochondria in the muscle, and IMF mitochondria to 81% [60]. In T1DM rats, the percentage of mtDNA each population rose in SS mitochondria and, lowered in IMF mitochondrial subpopulation, suggestive of increased SS biogenesis. The higher adaptability of SS mitochondria [60], might be an explanation for the T1DM-induced increase content of this mitochondrial subpopulation. For better comprehend these results, further analysis are needed, for example, the relative quantification through Western blot of proteins responsible for mtDNA biogenesis, like Tfam [88].

The BN-PAGE profile of SS and IMF mitochondrial subpopulations observed in the present study were different among each other (Figure 12). The noticeable feature is the presence of clearly more defined gel bands in IMF compared to SS subpopulation, with slight MW differences in each OXPHOS complex band. The OXPHOS profile of SS mitochondria noticed in BN-PAGE was different from the previously described [89], possibly justified by technical problems in the separation of SS mitochondria, which resulted in mitochondrial fractions of this subpopulation with lot of membranes and few mitochondria (Figure 11). On the other hand, no differences in the BN-PAGE profile were observed between the control and T1DM group, suggesting that OXPHOS assembly is not affected by T1DM. These results are supported by the western blot analysis of ATP synthase β, since no expression differences were observed between control and T1DM group (Figure 15). Regarding OXPHOS functionality, T1DM-induced decrease of ATP synthase activity was detected in SS mitochondria, being the opposite of the previous report of Baseler *et al*. [90]. Considering the control samples, no differences of OXPHOS complexes IV and V in-gel activities between IMF and SS subpopulations were noticed (Figure 13). These results are not in

accordance with a previous work [89], that reported a higher in-gel activity of CIV in IMF mitochondria, possibly justified by the low purity of SS subfractions.

As observed in Figure 13a, protein Quality Control (QC) system within mitochondria has a great importance in ATP synthesis and consequently in tissue bioenergetics [31]. The typical effector enzymes of protein homeostasis are molecular chaperones and proteases [91]. To evaluate the T1DM effect on mitochondrial proteolysis, gelatin zymography was performed (Figure 14). Two bands with activity were observed in SS and IMF mitochondria from CONT and T1DM groups in the zymography gel; however, the proteases present in those bands were not successfully identified by LC-MS/MS, due to technical problems. Nevertheless, considering the molecular weights, the protease present in the upper band might be Cathepsin, which has 29KDa, and was previously detected in human monocites, through gelatin zymography gel [92]. The protease present in the lower band might be a catalytic domain of Lon protease, since in a previous work from our group this peptide with ~15KDa was identified by LC-MS/MS in mitochondrial fractions (data not shown). Lon protease exists in the matrix with a function of degrading misfolded and non-assembled proteins and peptides in the matrix, including denaturated and carbonylated proteins, being aconitase a good example [93; 94]. Future work exploring the effect of T1DM on Lon expression will be relevant for a better comprehension of QC within mitochondria.

Among the mitochondrial proteases with QC function, the AAA^+ superfamily of ATPases have the task to fold and assembly unfolded and misfolded proteins that can accumulate in each of these four compartments [38]. The hetero-oligomeric m-AAA protease localized in the inner mitochondrial membrane [45], seem to be involved in the QC of inner membrane complexes [38]. To assess the effect of T1DM on m-AAA expression and relate it with OXPHOS organization and functionality, the expression of paraplegin, a subunit of m-AAA, was evaluated (Figure 16). An overexpression of paraplegin was observed in the SS mitochondrial subpopulation of diabetic rats, whereas lower levels were noticed in T1DM IMF subpopulation. An opposite profile was observed for the ratio of mitochondrial protein-to-mtDNA (Table 4), with lower values observed in T1DM SS mitochondria, and higher in the IMF subpopulation. Considering these two

observations and the fact that mitochondrial protein-to- mtDNA ratio gives a rough idea of the protein quantity per mitochondrion, the protein accumulation observed in IMF mitochondria from T1DM animals might be a consequence of the lower expression of m-AAA ATPases, or a lower QC proteins import within IMF mitochondria, as reported by Baseler *et al*. [90]. Since SS mitochondria are used to constant oxidative ambient [63], and adapt better and faster to pathophysiological conditions [67; 95], paraplegin overexpression can be seen as a SS response to T1DM, in order to eliminate damaged protein. In the other hand, the underexpression of paraplegin in IMF mitochondria from T1DM group might reflect the accumulation of misfolded and damaged proteins not eliminated due to the low levels of m-AAA, being paraplegin an important subunit of this QC system.

In overall, our results evidence a higher susceptibility of *gastrocnemius* IMF mitochondria to T1DM manifested by morphological and biochemical alterations.

5. Conclusions

In order to get a deep insight into the molecular mechanisms underlying type 1 diabetes complications-induced mitochondriopathy in skeletal muscle, the two mitochondrial subpopulations were isolated from *gastrocnemius* and morphologically and biochemically analysed. Data obtained allowed to conclude that:

- Four months of STZ treatment resulted in a notorious decrease of body and muscle mass compared to healthy animals, paralleled by significantly high glycemia and HbA1c levels.
- SS biogenesis increased in T1DM animals. Based on mtDNA–to-muscle mass ratio, a rough measure of mitochondrial content, an increment of SS mitochondrial content within *gastrocnemius* muscle was observed, whereas an opposite effect was noticed in IMF mitochondria, paralleled by a T1DM-related higher mitochondrial sectional area, lower levels of the cristae regulatory protein mitofilin and increased protein-to-mtDNA ratio, suggestive of protein accumulation within IMF mitochondria.
- OXPHOS complexes organization was not affected by T1DM, although mitochondrial functionality seems compromised, based on in-gel activity data.
- T1DM-related differences of the overall mitochondrial proteolytic activity were noticed, particularly notorious for IMF mitochondria, with significantly lower activity of a ~15KDa protease observed in diabetic rats. The levels of the subunit paraplegin from the m-AAA mitochondrial QC system were also lower in this mitochondrial population from diabetic animals. An opposite effect was observed for SS mitochondria.

Taken together, after four months of STZ administration, evidences of mitochondrial plasticity were noticed for both mitochondrial subpopulations from *gastrocnemius* muscle, especially regarding their biogenesis. IMF was the most

affected mitochondrial subpopulation in skeletal muscle regarding T1DM-induced dysfunction.

6. References

[1]J.E. Shaw, R.A. Sicree, P.Z. Zimmet, Global estimates of the prevalence of diabetes for 2010 and 2030. Diabetes Res Clin Pract 87 (2010) 4-14.
[2]S. Krause Mda, P.I. de Bittencourt, Jr., Type 1 diabetes: can exercise impair the autoimmune event? The L-arginine/glutamine coupling hypothesis. Cell Biochem Funct 26 (2008) 406-433.
[3]M. Mihanovic, D. Bodor, S. Kezic, B. Restek-Petrovic, A. Silic, Differential diagnosis of psychotropic side effects and symptoms and signs of psychiatric disorders. Psychiatr Danub 21 (2009) 570-574.
[4]J. Silverstein, G. Klingensmith, K. Copeland, L. Plotnick, F. Kaufman, L. Laffel, L. Deeb, M. Grey, B. Anderson, L.A. Holzmeister, N. Clark, Care of children and adolescents with type 1 diabetes: a statement of the American Diabetes Association. Diabetes Care 28 (2005) 186-212.
[5]A.E. Kitabchi, G.E. Umpierrez, J.M. Miles, J.N. Fisher, Hyperglycemic crises in adult patients with diabetes. Diabetes Care 32 (2009) 1335-1343.
[6]S.R. Patton, Adherence to diet in youth with type 1 diabetes. J Am Diet Assoc 111 (2011) 550-555.
[7]A.M. Jacobson, M. de Groot, J.A. Samson, The effects of psychiatric disorders and symptoms on quality of life in patients with type I and type II diabetes mellitus. Qual Life Res 6 (1997) 11-20.
[8]R.C. Lee, Z. Wang, M. Heo, R. Ross, I. Janssen, S.B. Heymsfield, Total-body skeletal muscle mass: development and cross-validation of anthropometric prediction models. Am J Clin Nutr 72 (2000) 796-803.
[9]T. Vellai, G. Vida, The origin of eukaryotes: the difference between prokaryotic and eukaryotic cells. Proc Biol Sci 266 (1999) 1571-1577.
[10]A.M. Distler, J. Kerner, C.L. Hoppel, Proteomics of mitochondrial inner and outer membranes. Proteomics 8 (2008) 4066-4082.
[11]M.W. Gray, G. Burger, B.F. Lang, Mitochondrial evolution. Science 283 (1999) 1476-1481.
[12]B.F. Lang, G. Burger, C.J. O'Kelly, R. Cedergren, G.B. Golding, C. Lemieux, D. Sankoff, M. Turmel, M.W. Gray, An ancestral mitochondrial DNA resembling a eubacterial genome in miniature. Nature 387 (1997) 493-497.
[13]S.G. Andersson, A. Zomorodipour, J.O. Andersson, T. Sicheritz-Ponten, U.C. Alsmark, R.M. Podowski, A.K. Naslund, A.S. Eriksson, H.H. Winkler, C.G. Kurland, The genome sequence of Rickettsia prowazekii and the origin of mitochondria. Nature 396 (1998) 133-140.
[14]C.J. Wallace, I. Clark-Lewis, A rationale for the absolute conservation of Asn70 and Pro71 in mitochondrial cytochromes c suggested by protein engineering. Biochemistry 36 (1997) 14733-14740.
[15]D.R. Green, Apoptotic pathways: the roads to ruin. Cell 94 (1998) 695-698.
[16]H.M. McBride, M. Neuspiel, S. Wasiak, Mitochondria: more than just a powerhouse. Curr Biol 16 (2006) R551-560.
[17]G. Hajnoczky, G. Csordas, S. Das, C. Garcia-Perez, M. Saotome, S. Sinha Roy, M. Yi, Mitochondrial calcium signalling and cell death: approaches for assessing the role of mitochondrial Ca2+ uptake in apoptosis. Cell Calcium 40 (2006) 553-560.
[18]G. Mathy, F.E. Sluse, Mitochondrial comparative proteomics: strengths and pitfalls. Biochim Biophys Acta 1777 (2008) 1072-1077.

[19]P.J. Adhihetty, V. Ljubicic, D.A. Hood, Effect of chronic contractile activity on SS and IMF mitochondrial apoptotic susceptibility in skeletal muscle. Am J Physiol Endocrinol Metab 292 (2007) E748-755.

[20]T.R. Koves, R.C. Noland, A.L. Bates, S.T. Henes, D.M. Muoio, R.N. Cortright, Subsarcolemmal and intermyofibrillar mitochondria play distinct roles in regulating skeletal muscle fatty acid metabolism. Am J Physiol Cell Physiol 288 (2005) C1074-1082.

[21]A.M. Aerts, P. Zabrocki, G. Govaert, J. Mathys, D. Carmona-Gutierrez, F. Madeo, J. Winderickx, B.P. Cammue, K. Thevissen, Mitochondrial dysfunction leads to reduced chronological lifespan and increased apoptosis in yeast. FEBS Lett 583 (2009) 113-117.

[22]J.W. Palmer, B. Tandler, C.L. Hoppel, Biochemical properties of subsarcolemmal and interfibrillar mitochondria isolated from rat cardiac muscle. J Biol Chem 252 (1977) 8731-8739.

[23]G. Attardi, G. Schatz, Biogenesis of mitochondria. Annu Rev Cell Biol 4 (1988) 289-333.

[24]M. Wang, X.C. Wang, Z.Y. Zhang, B. Mou, R.M. Hu, Impaired mitochondrial oxidative phosphorylation in multiple insulin-sensitive tissues of humans with type 2 diabetes mellitus. J Int Med Res 38 (2010) 769-781.

[25]R. Acin-Perez, P. Fernandez-Silva, M.L. Peleato, A. Perez-Martos, J.A. Enriquez, Respiratory active mitochondrial supercomplexes. Mol Cell 32 (2008) 529-539.

[26]G. Lenaz, M.L. Genova, Structural and functional organization of the mitochondrial respiratory chain: a dynamic super-assembly. Int J Biochem Cell Biol 41 (2009) 1750-1772.

[27]D.C. Gautheron, Mitochondrial oxidative phosphorylation and respiratory chain: review. J Inherit Metab Dis 7 Suppl 1 (1984) 57-61.

[28]R.A. Stuart, Supercomplex organization of the oxidative phosphorylation enzymes in yeast mitochondria. J Bioenerg Biomembr 40 (2008) 411-417.

[29]H. Schagger, Respiratory chain supercomplexes of mitochondria and bacteria. Biochim Biophys Acta 1555 (2002) 154-159.

[30]N.V. Dudkina, S. Sunderhaus, E.J. Boekema, H.P. Braun, The higher level of organization of the oxidative phosphorylation system: mitochondrial supercomplexes. J Bioenerg Biomembr 40 (2008) 419-424.

[31]T. Tatsuta, T. Langer, Quality control of mitochondria: protection against neurodegeneration and ageing. EMBO J 27 (2008) 306-314.

[32]G. Kroemer, L. Galluzzi, C. Brenner, Mitochondrial membrane permeabilization in cell death. Physiol Rev 87 (2007) 99-163.

[33]M. Koppen, T. Langer, Protein degradation within mitochondria: versatile activities of AAA proteases and other peptidases. Crit Rev Biochem Mol Biol 42 (2007) 221-242.

[34]S.A. Detmer, D.C. Chan, Functions and dysfunctions of mitochondrial dynamics. Nat Rev Mol Cell Biol 8 (2007) 870-879.

[35]J. Roth, G.H. Yam, J. Fan, K. Hirano, K. Gaplovska-Kysela, V. Le Fourn, B. Guhl, R. Santimaria, T. Torossi, M. Ziak, C. Zuber, Protein quality control: the who's who, the where's and therapeutic escapes. Histochem Cell Biol 129 (2008) 163-177.

[36]S.H. Park, N. Bolender, F. Eisele, Z. Kostova, J. Takeuchi, P. Coffino, D.H. Wolf, The cytoplasmic Hsp70 chaperone machinery subjects misfolded and endoplasmic reticulum import-incompetent proteins to degradation via the ubiquitin-proteasome system. Mol Biol Cell 18 (2007) 153-165.

[37]B. Friguet, A.L. Bulteau, I. Petropoulos, Mitochondrial protein quality control: implications in ageing. Biotechnol J 3 (2008) 757-764.

[38]B.M. Baker, C.M. Haynes, Mitochondrial protein quality control during biogenesis and aging. Trends Biochem Sci 36 (2011) 254-261.

[39]K. Leonhard, B. Guiard, G. Pellecchia, A. Tzagoloff, W. Neupert, T. Langer, Membrane protein degradation by AAA proteases in mitochondria: extraction of substrates from either membrane surface. Mol Cell 5 (2000) 629-638.

[40]H. Arlt, R. Tauer, H. Feldmann, W. Neupert, T. Langer, The YTA10-12 complex, an AAA protease with chaperone-like activity in the inner membrane of mitochondria. Cell 85 (1996) 875-885.

[41]M. Koppen, F. Bonn, S. Ehses, T. Langer, Autocatalytic processing of m-AAA protease subunits in mitochondria. Mol Biol Cell 20 (2009) 4216-4224.

[42]K. Leonhard, J.M. Herrmann, R.A. Stuart, G. Mannhaupt, W. Neupert, T. Langer, AAA proteases with catalytic sites on opposite membrane surfaces comprise a proteolytic system for the ATP-dependent degradation of inner membrane proteins in mitochondria. EMBO J 15 (1996) 4218-4229.

[43]M. Nolden, S. Ehses, M. Koppen, A. Bernacchia, E.I. Rugarli, T. Langer, The m-AAA protease defective in hereditary spastic paraplegia controls ribosome assembly in mitochondria. Cell 123 (2005) 277-289.

[44]K. Esser, B. Tursun, M. Ingenhoven, G. Michaelis, E. Pratje, A novel two-step mechanism for removal of a mitochondrial signal sequence involves the mAAA complex and the putative rhomboid protease Pcp1. J Mol Biol 323 (2002) 835-843.

[45]E.I. Rugarli, T. Langer, Translating m-AAA protease function in mitochondria to hereditary spastic paraplegia. Trends Mol Med 12 (2006) 262-269.

[46]T. Karlberg, S. van den Berg, M. Hammarstrom, J. Sagemark, I. Johansson, L. Holmberg-Schiavone, H. Schuler, Crystal structure of the ATPase domain of the human AAA+ protein paraplegin/SPG7. PLoS One 4 (2009) e6975.

[47]K. Karata, T. Inagawa, A.J. Wilkinson, T. Tatsuta, T. Ogura, Dissecting the role of a conserved motif (the second region of homology) in the AAA family of ATPases. Site-directed mutagenesis of the ATP-dependent protease FtsH. J Biol Chem 274 (1999) 26225-26232.

[48]M. Nolden, B. Kisters-Woike, T. Langer, M. Graef, Quality control of proteins in the mitochondrion, in: I. Braakman, (Ed.), Chaperones, Springer Berlin / Heidelberg, 2006, pp. 119-147.

[49]N. Ishihara, Y. Fujita, T. Oka, K. Mihara, Regulation of mitochondrial morphology through proteolytic cleavage of OPA1. EMBO J 25 (2006) 2966-2977.

[50]J.Y. Mun, T.H. Lee, J.H. Kim, B.H. Yoo, Y.Y. Bahk, H.S. Koo, S.S. Han, Caenorhabditis elegans mitofilin homologs control the morphology of mitochondrial cristae and influence reproduction and physiology. J Cell Physiol 224 (2010) 748-756.

[51]S. Ehses, I. Raschke, G. Mancuso, A. Bernacchia, S. Geimer, D. Tondera, J.C. Martinou, B. Westermann, E.I. Rugarli, T. Langer, Regulation of OPA1 processing and mitochondrial fusion by m-AAA protease isoenzymes and OMA1. J Cell Biol 187 (2009) 1023-1036.

[52]C. Merkwirth, S. Dargazanli, T. Tatsuta, S. Geimer, B. Lower, F.T. Wunderlich, J.C. von Kleist-Retzow, A. Waisman, B. Westermann, T. Langer, Prohibitins control cell proliferation and apoptosis by regulating OPA1-dependent cristae morphogenesis in mitochondria. Genes Dev 22 (2008) 476-488.

[53]G.B. John, Y. Shang, L. Li, C. Renken, C.A. Mannella, J.M. Selker, L. Rangell, M.J. Bennett, J. Zha, The mitochondrial inner membrane protein mitofilin controls cristae morphology. Mol Biol Cell 16 (2005) 1543-1554.

[54]J. Xie, M.F. Marusich, P. Souda, J. Whitelegge, R.A. Capaldi, The mitochondrial inner membrane protein mitofilin exists as a complex with SAM50, metaxins 1 and 2, coiled-coil-helix coiled-coil-helix domain-containing protein 3 and 6 and DnaJC11. FEBS Lett 581 (2007) 3545-3549.

[55]C. Gieffers, F. Korioth, P. Heimann, C. Ungermann, J. Frey, Mitofilin is a transmembrane protein of the inner mitochondrial membrane expressed as two isoforms. Exp Cell Res 232 (1997) 395-399.

[56]G. Biolo, A. Gastaldelli, X.J. Zhang, R.R. Wolfe, Protein synthesis and breakdown in skin and muscle: a leg model of amino acid kinetics. Am J Physiol 267 (1994) E467-474.

[57]H. Westerblad, J.D. Bruton, A. Katz, Skeletal muscle: energy metabolism, fiber types, fatigue and adaptability. Exp Cell Res 316 (2010) 3093-3099.

[58]G.A. Dudley, P.C. Tullson, R.L. Terjung, Influence of mitochondrial content on the sensitivity of respiratory control. J Biol Chem 262 (1987) 9109-9114.

[59]M. Koppen, M.D. Metodiev, G. Casari, E.I. Rugarli, T. Langer, Variable and tissue-specific subunit composition of mitochondrial m-AAA protease complexes linked to hereditary spastic paraplegia. Mol Cell Biol 27 (2007) 758-767.

[60]P.J. Adhihetty, V. Ljubicic, K.J. Menzies, D.A. Hood, Differential susceptibility of subsarcolemmal and intermyofibrillar mitochondria to apoptotic stimuli. Am J Physiol Cell Physiol 289 (2005) C994-C1001.

[61]M. Takahashi, D.A. Hood, Protein import into subsarcolemmal and intermyofibrillar skeletal muscle mitochondria. Differential import regulation in distinct subcellular regions. J Biol Chem 271 (1996) 27285-27291.

[62]R. Ferreira, R. Vitorino, R.M. Alves, H.J. Appell, S.K. Powers, J.A. Duarte, F. Amado, Subsarcolemmal and intermyofibrillar mitochondria proteome differences disclose functional specializations in skeletal muscle. Proteomics 10 (2010) 3142-3154.

[63]A.V. Kuznetsov, J. Troppmair, R. Sucher, M. Hermann, V. Saks, R. Margreiter, Mitochondrial subpopulations and heterogeneity revealed by confocal imaging: possible physiological role? Biochim Biophys Acta 1757 (2006) 686-691.

[64]P.J. Adhihetty, I. Irrcher, A.M. Joseph, V. Ljubicic, D.A. Hood, Plasticity of skeletal muscle mitochondria in response to contractile activity. Exp Physiol 88 (2003) 99-107.

[65]A. Riva, B. Tandler, F. Loffredo, E. Vazquez, C. Hoppel, Structural differences in two biochemically defined populations of cardiac mitochondria. Am J Physiol Heart Circ Physiol 289 (2005) H868-872.

[66]V.P. Skulachev, Mitochondrial filaments and clusters as intracellular power-transmitting cables. Trends Biochem Sci 26 (2001) 23-29.

[67]D.A. Hood, Invited Review: contractile activity-induced mitochondrial biogenesis in skeletal muscle. J Appl Physiol 90 (2001) 1137-1157.

[68]A. Bonetto, F. Penna, M. Muscaritoli, V.G. Minero, F. Rossi Fanelli, F.M. Baccino, P. Costelli, Are antioxidants useful for treating skeletal muscle atrophy? Free Radic Biol Med 47 (2009) 906-916.

[69]J.A. Lumini, J. Magalhaes, P.J. Oliveira, A. Ascensao, Beneficial effects of exercise on muscle mitochondrial function in diabetes mellitus. Sports Med 38 (2008) 735-750.

[70]O. Savu, V.G. Sunkari, I.R. Botusan, J. Grunler, A. Nikolsjkov, S.B. Catrina, Stability of mitochondrial DNA against reactive oxygen species (ROS) generated in diabetes. Diabetes Metab Res Rev (2011).

[71]J. Hur, K.A. Sullivan, A.D. Schuyler, Y. Hong, M. Pande, D.J. States, H.V. Jagadish, E.L. Feldman, Literature-based discovery of diabetes- and ROS-related targets. BMC Med Genomics 3 (2010) 49.

[72]K. Morino, K.F. Petersen, S. Dufour, D. Befroy, J. Frattini, N. Shatzkes, S. Neschen, M.F. White, S. Bilz, S. Sono, M. Pypaert, G.I. Shulman, Reduced mitochondrial density and increased IRS-1 serine phosphorylation in muscle of insulin-resistant offspring of type 2 diabetic parents. J Clin Invest 115 (2005) 3587-3593.

[73]T.T. Chao, C.D. Ianuzzo, R.B. Armstrong, J.T. Albright, S.E. Anapolle, Ultrastructural alterations in skeletal muscle fibers of streptozotocin-diabetic rats. Cell Tissue Res 168 (1976) 239-246.

[74]U.M. Marinari, R. Monacelli, D. Cottalasso, A. Novelli, Effects of alloxan diabetes and insulin on morphology and certain functional activities of mitochondria of the rat liver and heart. Acta Diabetol Lat 11 (1974) 296-314.

[75]H. Bugger, S. Boudina, X.X. Hu, J. Tuinei, V.G. Zaha, H.A. Theobald, U.J. Yun, A.P. McQueen, B. Wayment, S.E. Litwin, E.D. Abel, Type 1 diabetic akita mouse hearts are insulin sensitive but manifest structurally abnormal mitochondria that remain coupled despite increased uncoupling protein 3. Diabetes 57 (2008) 2924-2932.

[76]N. Cester, R.A. Rabini, E. Salvolini, R. Staffolani, A. Curatola, A. Pugnaloni, M.A. Brunelli, G. Biagini, L. Mazzanti, Activation of endothelial cells during insulin-dependent diabetes mellitus: a biochemical and morphological study. Eur J Clin Invest 26 (1996) 569-573.

[77]H. Haacke, [Induction of diabetes mellitus of various degree of severity using streptozotocin in rats]. Klin Wochenschr 47 (1969) 437-438.

[78]H. Schagger, G. von Jagow, Blue native electrophoresis for isolation of membrane protein complexes in enzymatically active form. Anal Biochem 199 (1991) 223-231.

[79]E. Zerbetto, L. Vergani, F. Dabbeni-Sala, Quantification of muscle mitochondrial oxidative phosphorylation enzymes via histochemical staining of blue native polyacrylamide gels. Electrophoresis 18 (1997) 2059-2064.

[80]C. Martineau, [Diabetes mellitus, a stammering epidemic]. Soins (2008) S1.

[81]A. Martinez-Castelao, [Clinical and social impact of the diabetes mellitus epidemic]. Nefrologia 28 (2008) 245-248.

[82]R. Ostermann-Myrau, [Diabetes mellitus: an epidemic rise?]. Versicherungsmedizin 60 (2008) 63-65.

[83]M. Elsner, B. Guldbakke, M. Tiedge, R. Munday, S. Lenzen, Relative importance of transport and alkylation for pancreatic beta-cell toxicity of streptozotocin. Diabetologia 43 (2000) 1528-1533.

[84]J. Lumini-Oliveira, J. Magalhaes, C.V. Pereira, A.C. Moreira, P.J. Oliveira, A. Ascensao, Endurance training reverts heart mitochondrial dysfunction, permeability transition and apoptotic signaling in long-term severe hyperglycemia. Mitochondrion 11 (2011) 54-63.

[85]T. Szkudelski, The mechanism of alloxan and streptozotocin action in B cells of the rat pancreas. Physiol Res 50 (2001) 537-546.

[86]F. Ferreirinha, A. Quattrini, M. Pirozzi, V. Valsecchi, G. Dina, V. Broccoli, A. Auricchio, F. Piemonte, G. Tozzi, L. Gaeta, G. Casari, A. Ballabio, E.I. Rugarli, Axonal degeneration in paraplegin-deficient mice is associated with abnormal mitochondria and impairment of axonal transport. J Clin Invest 113 (2004) 231-242.

[87]C. Frezza, S. Cipolat, O. Martins de Brito, M. Micaroni, G.V. Beznoussenko, T. Rudka, D. Bartoli, R.S. Polishuck, N.N. Danial, B. De Strooper, L. Scorrano, OPA1 controls apoptotic cristae remodeling independently from mitochondrial fusion. Cell 126 (2006) 177-189.

[88]B. Chabi, P.J. Adhihetty, V. Ljubicic, D.A. Hood, How is mitochondrial biogenesis affected in mitochondrial disease? Med Sci Sports Exerc 37 (2005) 2102-2110.

[89]A.I. Padrao, R.M. Ferreira, R. Vitorino, R.M. Alves, M.J. Neuparth, J.A. Duarte, F. Amado, OXPHOS susceptibility to oxidative modifications: The role of heart mitochondrial subcellular location. Biochim Biophys Acta (2011).

[90]W.A. Baseler, E.R. Dabkowski, C.L. Williamson, T.L. Croston, D. Thapa, M.J. Powell, T.T. Razunguzwa, J.M. Hollander, Proteomic alterations of distinct mitochondrial

subpopulations in the type 1 diabetic heart: contribution of protein import dysfunction. Am J Physiol Regul Integr Comp Physiol 300 (2011) R186-200.

[91]T. Bender, C. Leidhold, T. Ruppert, S. Franken, W. Voos, The role of protein quality control in mitochondrial protein homeostasis under oxidative stress. Proteomics 10 (2010) 1426-1443.

[92]W.A. Li, Z.T. Barry, J.D. Cohen, C.L. Wilder, R.J. Deeds, P.M. Keegan, M.O. Platt, Detection of femtomole quantities of mature cathepsin K with zymography. Anal Biochem 401 (2010) 91-98.

[93]D.A. Bota, J.K. Ngo, K.J. Davies, Downregulation of the human Lon protease impairs mitochondrial structure and function and causes cell death. Free Radic Biol Med 38 (2005) 665-677.

[94]E. Gur, R.T. Sauer, Recognition of misfolded proteins by Lon, a AAA(+) protease. Genes Dev 22 (2008) 2267-2277.

[95]H. Hoppeler, Exercise-induced ultrastructural changes in skeletal muscle. Int J Sports Med 7 (1986) 187-204.